②

WRDC-TR-89-2038

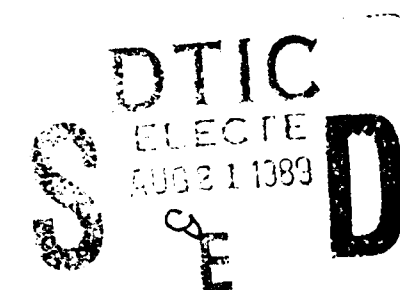# PHASE CHANGE MATERIAL FOR SPACECRAFT THERMAL MANAGEMENT

J. W. Sheffield, Ph.D.
C. Wen, M.S.

Mechanical and Aerospace Engineering
and Engineering Mechanics
University of Missouri-Rolla
Rolla, MO 65401-0249

AD-A211 404

April 1989

Interim Report for Period March 1987 - March 1988

Approved for public release; distribution unlimited.

DTIC
ELECTE
AUG 21 1989
S E D

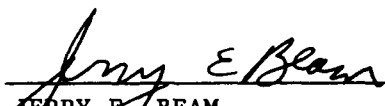89 8 21 015

NOTICE

When Government drawings, specifications, or other data are used for any purpose other than in connection with a definitely Government-related procurement, the United States Government incurs no responsibility or any obligation whatsoever. The fact that the government may have formulated or in any way supplied the said drawings, specifications, or other data, is not to be regarded by implication, or otherwise in any manner construed, as licensing the holder, or any other person or corporation; or as conveying any rights or permission to manufacture, use, or sell any patented invention that may in any way be related thereto.

This report is releasable to the National Technical Information Service (NTIS). At NTIS, it will be available to the general public, including foreign nations.

This technical report has been reviewed and is approved for publication.

JOHN E. LELAND
Power Technology Branch
Aerospace Power Division
Aero Propulsion and Power Laboratory

JERRY E. BEAM
Power Technology Branch
Aerospace Power Division
Aero Propulsion and Power Laboratory

FOR THE COMMANDER

WILLIAM U. BORGER
Chief, Aerospace Power Division
Aero Propulsion & Power Laboratory

If your address has changed, if you wish to be removed from our mailing list, or if the addressee is no longer employed by your organization please notify WRDC/POOS, WPAFB, OH 45433-6563 to help us maintain a current mailing list.

Copies of this report should not be returned unless return is required by security considerations, contractual obligations, or notice on a specific document.

REPORT DOCUMENTATION PAGE

Form Approved
OMB No. 0704-0188

1a. REPORT SECURITY CLASSIFICATION	1b. RESTRICTIVE MARKINGS
Unclassified	N/A

2a. SECURITY CLASSIFICATION AUTHORITY	3. DISTRIBUTION/AVAILABILITY OF REPORT
N/A	Approved for public release; distribution unlimited
2b. DECLASSIFICATION/DOWNGRADING SCHEDULE	
N/A	

4. PERFORMING ORGANIZATION REPORT NUMBER(S)	5. MONITORING ORGANIZATION REPORT NUMBER(S)
	WRDC-TR-89-2038

6a. NAME OF PERFORMING ORGANIZATION	6b. OFFICE SYMBOL (If applicable)	7a. NAME OF MONITORING ORGANIZATION
University of Missouri-Rolla		Aero Propulsion and Power Laboratory WRDC, AFSC

6c. ADDRESS (City, State, and ZIP Code)	7b. ADDRESS (City, State, and ZIP Code)
Rolla, MO 65401-0249	WRDC/POOS-3 Wright-Patterson AFB OH 45433-6563

8a. NAME OF FUNDING/SPONSORING ORGANIZATION	8b. OFFICE SYMBOL (If applicable)	9. PROCUREMENT INSTRUMENT IDENTIFICATION NUMBER
		F33615-86-C-2721

8c. ADDRESS (City, State, and ZIP Code)	10. SOURCE OF FUNDING NUMBERS			
	PROGRAM ELEMENT NO.	PROJECT NO.	TASK NO.	WORK UNIT ACCESSION NO.
	62203F	3145	20	49

11. TITLE (Include Security Classification)

Phase Change Material for Spacecraft Thermal Management

12. PERSONAL AUTHOR(S)

Sheffield, J. W., and Wen, C.

13a. TYPE OF REPORT	13b. TIME COVERED	14. DATE OF REPORT (Year, Month, Day)	15. PAGE COUNT
Interim	FROM 15Mar87 TO 31Mar88	1989 April	72

16. SUPPLEMENTARY NOTATION

17. COSATI CODES			18. SUBJECT TERMS (Continue on reverse if necessary and identify by block number)
FIELD	GROUP	SUB-GROUP	Phase Change Material
22	07		Thermal Storage
			Spacecraft Thermal Control. (cd.)

19. ABSTRACT (Continue on reverse if necessary and identify by block number)

Heat transfer problems involving phase change are encountered extensively in technical and natural processes. Latent heat storage systems, which possess the advantages of high density of energy and isothermal behavior during charging and discharging, is one application of using phase change material (PCM). A computational model is presented for the prediction of the heat transfer between a heat transfer fluid (HTF) and a phase change material (PCM) of a latent heat storage unit. Two models of flow, hydrodynamically fully developed flow and developing flow, of the HTF were proposed in this study. A two-dimensional enthalpy method was used for the computation of the phase change heat transfer in the PCM. A fully implicit finite difference scheme was utilized for the calculation of convective heat transfer in the HTF. The unknown time dependent boundary condition between the HTF and the PCM was found iteratively. The predictions are substantiated by their fair agreement with experimental data. Factors which affect the heat transfer rates between the HTF and the PCM were studied numerically for both hydrodynamically fully developed flow and developing flow. It is found that the Nusselt number is significantly increased by the developing temperature profiles.

20. DISTRIBUTION/AVAILABILITY OF ABSTRACT	21. ABSTRACT SECURITY CLASSIFICATION
☐ UNCLASSIFIED/UNLIMITED ☐ SAME AS RPT. ☒ DTIC USERS	UNCLASSIFIED

22a. NAME OF RESPONSIBLE INDIVIDUAL	22b. TELEPHONE (Include Area Code)	22c. OFFICE SYMBOL
J. E. Leland	513-255-6241	WRDC/POOS-3

DD Form 1473, JUN 86   Previous editions are obsolete.   SECURITY CLASSIFICATION OF THIS PAGE

FOREWORD

The information presented in this report was generated during the performance of the Task No. 4 of AF Contract F33615-86-C-2721. The technical work was carried out at the University of Missouri-Rolla, Department of Mechanical and Aerospace Engineering.

Dr. John W. Sheffield served as the principal investigator of the program. Michael P. O'Dell and Chudong Wen were the graduate students supported by this contract. This is a status report which presents the results generated during the period of is 1 March 1987 to 31 March 1988. The program was sponsored by the Aeronautical Systems Division of the Air Force with Mr. John E. Leland of the Aero Propulsion and Power Laboratory, WRDC/POOS, Wright-Patterson AFB, Ohio 45433-6563, serving as the technical monitor.

Accession For

NTIS GRA&I	X	
DTIC TAB	☐	
Unannounced	☐	
Justification		

By_____
Distribution/
Availability Codes

Dist	Avail and/or Special
A-1	

TABLE OF CONTENTS

TABLE OF CONTENTS (Continued)

LIST OF FIGURES

LIST OF TABLES

I. INTRODUCTION

The high power requirements of future spacecraft missions present many technological challenges to the designers of spacecraft thermal management systems (SCTMS). The need to buffer thermal loads, such as during burst power conditions, is presently a major problem. One possible solution is the application of latent heat storage with its use of phase change materials (PCM) to buffer the large heat input conditions. The present investigation was motivated by the need for predictive tools necessary for the design of SCTMS utilizing latent thermal energy storage. In this research, a latent heat storage unit is configured as shown in Fig. 1. The PCM is contained in a long horizontal tube assembled within a cylindrical shell. The temperature controlled heat transfer fluid (HTF) is pumped through the shell-and-tube heat exchanger to release or absorb thermal energy to or from the PCM.
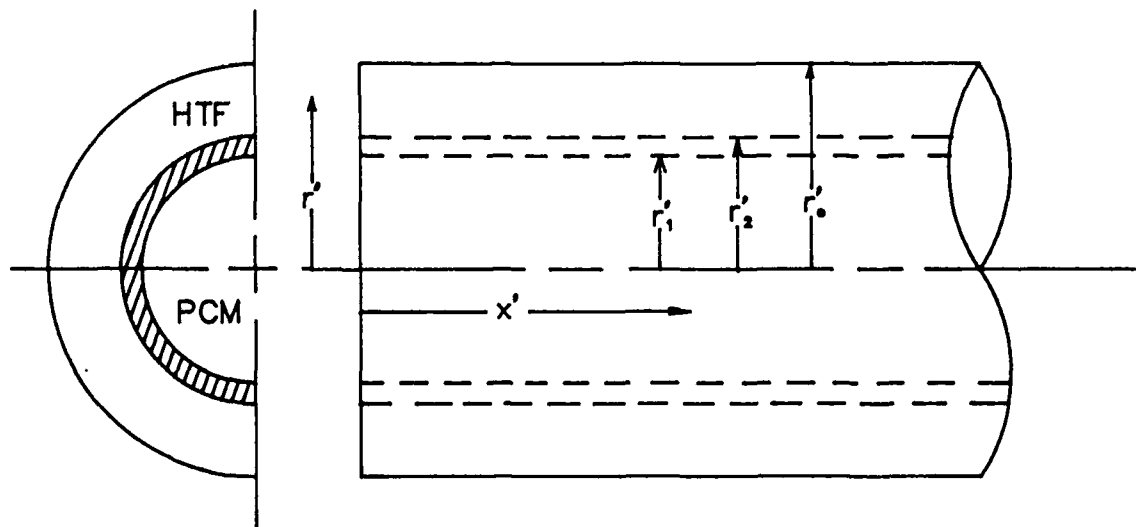
Figure 1. Latent Heat Storage Unit and Coordinate System

Basically, the analysis of heat transfer in this latent heat storage unit is divided into two problems: the melting/freezing problem of the PCM in a horizontal tube and the convective heat transfer problem of the HTF in an annular passage.

For the present melting/freezing problem, the unknown tube wall temperature is assumed to be time and location dependent. This problem is rather difficult to solve due to the moving boundary and the unknown wall temperature. By introducing the enthalpy method, this problem becomes much simpler. The governing equation of the enthalpy method is similar to the single phase conduction equation. Using the enthalpy method to approach a phase change problem has the following advantages: (1) there are no conditions to be satisfied at the phase change boundary; (2) there is no need to accurately track the phase change boundary; (3) there is no need to consider the solid and the liquid sides separately; and (4) it allows a mushy zone between solid and liquid phases. The unknown tube wall temperature between the heat transfer fluid and the PCM is obtained from an energy balance. However, an iterative procedure is required. The Newton-Raphson method is used for this "root-finding" problem.

One of the objectives of this research is to develop a numerical method to find the heat transfer between the HTF and the PCM. The comprehensive understanding of the heat transfer in the latent heat storage system can provide the information for the design of spacecraft thermal management systems. However, there are many other important applications, such as metal casting, crystal growth, and thermal energy storage for building space conditioning, where the fundamental understanding of the phase change phenomena is important.

II. BACKGROUND

A. MELTING/FREEZING HEAT TRANSFER IN HORIZONTAL CYLINDERS

The heat transfer processes which occur during melting/freezing in horizontal cylinders have recently received considerable attention due to a wide range of engineering applications. Mathematically, the problem belongs to the "moving boundary" class of problems, which are difficult to find analytical solutions. Webb and co-workers [1] studied the melting phenomenology of water in a horizontal cylindrical capsule by experiment. The solid-liquid interface and the interaction of fluid flow, due to natural convection and the motion of the solid induced by the density inversion of the water-ice system, were determined visually. Heat transfer at the solid-liquid interface during melting from a horizontal cylindrical heat source embedded in a PCM was studied by Bathelt and Viskanta [2]. Two paraffins, n-heptadecane, $T_f = 22.2°C$ and n-octadecane, $T_f = 28.2°C$ were used as the PCMs. The shape of the solid-liquid interface was determined photographically, and the local heat transfer coefficients were measured using a shadowgraph technique. Ho [3] and Pannu [4] used the vorticity-stream function method to deal with the problem of phase change in horizontal cylinders. This method is based on the consideration that the heat transfer in the liquid PCM is by natural convection. A perturbation method was used by Yao [5] to solve the melting problem in a horizontal cylinder. This method is complex, tedious and limited to small Stefan numbers. Rieger et al. [6,7] used a numerically generated coordinate system, which conformed to the shape of the boundaries, to study the melting process around a horizontal cylinder. Due to the changing shape of the solid-liquid interface, this method appears to be laborious.

All the aforementioned studies did not consider the temperature variation of the PCM in the axial direction. Also, most are limited to uniform tube wall temperature. Experimental studies have also focussed on the control of the tube wall temperature

3

to be uniform. McCabe [8] obtained numerical solutions for time dependent temperature distributions. 'Ie used the enthalpy method with an implicit scheme to solve the melting/freezing problem in cylinders. However, only radial solutions were obtained. Like the other authors, he also did not take the axial dependence into account. In terms of the conjugate heat transfer problems problems inmolving the IITF and the PCM with "natural" boundary conditions at the interface, several papers [9 − 11] have addressed the problem of freezing on the outside of horizontal cylinder.

B. HEAT TRANSFER IN ANNULAR PASSAGES

The annulus represents a common geometry employed in a variety of heat transfer systems ranging from simple heat exchangers to the most complicated nuclear reactors. Theoretical and numerical studies of heat transfer in an annulus can be roughly divided into two types: heat transfer in a hydrodynamically fully developed region and heat transfer in an entry region.

1. Heat Transfer in Hydrodynamically Fully Developed Region. For the case of an axially symmetric hydrodynamically fully developed fluid flow with constant properties in a concentric annulus, Reynolds et al. [12] concluded that there are four types of fundamental boundary conditions of interest: (1) a step temperature on one wall and the other wall maintained at the inlet temperature, (2) uniform heat flux at one wall and the other wall being kept adiabatic, (3) uniform wall temperature at one wall and the other wall remaining insulated, and (4) uniform heat flux from one wall with the opposite wall maintained at the inlet temperature. A very thorough treatment of the annulus problem has been published by Lundberg et al. [13] based on these four types of fundamental solutions. They used an eigenvalue method to yield an exact solution for the entire thermal entrance region, but near the point of a step-change in either the wall temperature or the heat flux at the wall, a large number of terms in the

eigenfunction expansion are required. Worsoe-Schmidt [14] obtained these four types of fundamental solutions by using a similarity transformation method. The similarity variable used was obtained from Leveque solution. Hatton and Quarmby [15] also used the eigenvalue method to find solutions of heat transfer in annuli. However, only the cases with either uniform wall temperature or uniform heat flux on the inside wall and with the outside wall insulated were analyzed. The case of an arbitrarily prescribed heat flux around the periphery of either wall, or both walls, was studied by Sutherland et al. [16]. The technique used was an expansion of the known peripheral heat flux distribution in a Fourier series. Because the resulting temperature distribution can also be expressed as a Fourier series, the energy equation becomes a set of ordinary differential equations in terms of the eigenfunction. These eigenfunctions were used with the Fourier coefficients of any peripheral heat flux distribution to obtain the resulting wall temperature distribution.

2. <u>Heat Transfer in Entry Region</u>. The solution of the heat transfer problem with simultaneously development of velocity and temperature fields has been the subject of a great deal of attention during the past three decades. Due to the fact that the temperature profile cannot be obtained without knowing the velocity profile, the solution is usually obtained by first solving the hydrodynamic entry length problem, and then solving the thermal entry length problem.

Murakawa [17] has obtained an approximate entrance length solution for the annulus via a series solution. The final result only partially satisfies the boundary conditions. Liron et al. [18] also obtained solutions for flow in an annular region by representing the momentum equation by the stream function and then by using an eigenvalue method. However, the solution is restricted to vanishingly small Reynolds numbers. Heaton et al. [19] obtained a velocity profile defined over the entire region by linearizing the momentum equation and solving the resulting equations analytically.

For the thermal entry length problem, Murakawa [17] has obtained a solution for an arbitrary wall temperature at the inner wall of the annulus by an integral method. The developing velocity and temperature profiles used were simplified and was only applicable near the inner wall. The resulting solution did not show all the geometric effects nor did it approach the fully developed solution. Heaton et al. [19] linearized the energy equation to find the temperature profile. Their solution was obtained by an integral method. However, the only solution obtained was the case of uniform heat flux at one wall and the other wall insulated.

III. ANALYSIS

A. ENTHALPY MODEL FOR PHASE CHANGE PROBLEM

For an arbitrary control volume V which is fixed in space and if conduction is the only heat transfer mechanism to be considered, the time rate of change of internal energy has to be equal to the net rate at which heat is conducted through V if there is no energy source inside V and no external work toward V. Mathematically, this can be expressed by the following:

$$\frac{d}{dt}\int_V \rho U \, dV = \int_A k\, \nabla T \cdot \hat{n}\, dA \qquad (1)$$

Note that in the absence of motion, the pressure, P, is independent of time. Thus

$$\frac{d}{dt}\int_V P \, dV = 0 \qquad (2)$$

Since

$$\rho U = \rho i - P \qquad (3)$$

Equation (1) can be written in the form

$$\frac{d}{dt}\int_V \rho i \, dV = \int_A k\, \nabla T \cdot \hat{n}\, dA \qquad (4)$$

Equation (4) is the general form of enthalpy equation. The $i - versus - T$ relationship for the phase change material is used in conjuction with Eq. (4). Frequently, the dimensionless enthalpy, θ, is defined as

$$\theta = \frac{1}{\rho V} \int_0^V \frac{\rho(i - i_l^*)}{\lambda} \, dV \tag{5}$$

For the case of melting/freezing process in a horizontal tube, θ, for the control volume as shown in Fig. 2 , is

$$\theta = \frac{2}{\rho \, (r'^2_{i+1} - r'^2_i) \, \Delta x'} \int_0^V \rho \frac{(i - i_l^*)}{\lambda} \, dV \tag{6}$$

if the buoyancy effect in the liquid PCM is neglected and the density is assumed to be constant.

Introducing θ, Fo, and ϕ, where

$$Fo = \frac{\alpha t}{r'^2_1} \tag{7}$$

and

$$\phi = \frac{C_p (T - T_l^*)}{\lambda} \tag{8}$$

into Eq. (4), one has

$$\frac{\partial \theta}{\partial Fo}\bigg|_{i,j} = \left(\frac{\partial \phi}{\partial \chi}\bigg|_{i,j+1} - \frac{\partial \phi}{\partial \chi}\bigg|_{i,j} \right) \frac{1}{\Delta \chi} + \frac{2}{r^2_{i+1} - r^2_i} \left(\frac{\partial \phi}{\partial r}\bigg|_{i+1,j} \cdot r_{i+1} - \frac{\partial \phi}{\partial r}\bigg|_{i,j} \cdot r_i \right) \tag{9}$$

8

Forward difference in time and backward difference in space, the explicit finite-difference representation of Eq. (9) is

$$
\frac{\theta_{i,j}^{m+1} - \theta_{i,j}^{m}}{\Delta Fo} = \frac{\phi_{i,j+1}^{m} + \phi_{i,j-1}^{m} - 2\phi_{i,j}^{m}}{\Delta\chi^2}
$$

$$
+ \frac{2}{r_{i+1} + r_i} \frac{[(\phi_{i+1,j}^{m} - \phi_{i,j}^{m})r_{i+1} - (\phi_{i,j}^{m} - \phi_{i-1,j}^{m})r_i]}{\Delta r^2} \qquad (10)
$$

The relationships between θ and ϕ are

$$\phi = \theta \qquad \text{when} \quad \theta \geq 0 \qquad\qquad (11a)$$

$$\phi = 0 \qquad \text{when} \quad -1 \leq \theta \leq 0 \qquad\qquad (11b)$$

$$\phi = \theta + 1 \qquad \text{when} \quad \theta < -1 \qquad\qquad (11c)$$

Equation (10) should be used in conjuction with the energy equation and the momentum equation for the HTF, since the conditions between the HTF and the PCM are functions of time and location. Due to the unknown temperature boundary condition between the PCM and the HTF, the implicit scheme of the finite-difference equation for the enthalpy model appears to be inappropriate. The explicit scheme is therefore used since it is the more straightforward method.

B. HEAT TRANSFER IN AN ANNULAR PASSAGE

The current problem of interest is heat transfer in an annular passage with a transient temperature distribution. The dimensionless differential equations associated with this problem are the continuity equation, the momentum equation, and the energy equation as given below:

9
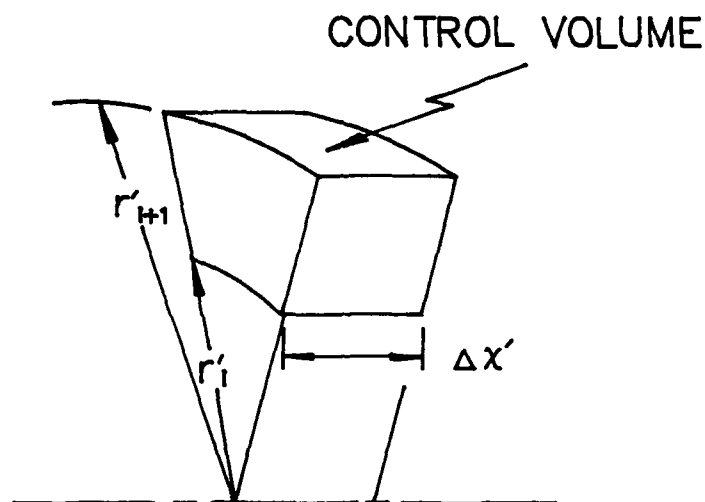
Figure 2.   Control Volume in Cylindrical coordinates

$$\frac{\partial u}{\partial x} + \frac{1}{r}\frac{\partial(rv)}{\partial r} = 0 \tag{12}$$

$$u\frac{\partial u}{\partial x} + v\frac{\partial u}{\partial r} = -\frac{1}{2}\frac{dp}{dx} + 2(\frac{\partial^2 u}{\partial r^2} + \frac{1}{r}\frac{\partial u}{\partial r}) \tag{13}$$

$$\frac{\partial T}{\partial \tau} + \frac{Pr}{2}(u\frac{\partial T}{\partial x} + v\frac{\partial T}{\partial r}) = \frac{\partial^2 T}{\partial r^2} + \frac{1}{r}\frac{\partial T}{\partial r} \tag{14}$$

These equations assume steady, laminar, incompressible flow with constant fluid properties and negligible axial conduction, buoyancy effect, internal energy generation, viscous energy dissipation, and axial rate of change of the radial shear stress. However,

for the current problem, the flowing fluid temperature is time dependent. Therefore, the the energy equation is transient. The boundary conditions for these equations are given by the following:

$$u(x, r_2) = v(x, r_2) = 0 \qquad (15)$$

$$u(x, 1) = v(x, 1) = 0 \qquad (16)$$

$$u(0, r) = u_e(r) \qquad (17)$$

$$T(\tau, x, r_2) = T_2(\tau, x) \qquad (18)$$

$$\frac{\partial T(\tau, x, 1)}{\partial r} = 0 \qquad (19)$$

$$T(\tau, 0, r) = T_e(t) \qquad (20)$$

Equation (19) indicates that the shell is insulated at $r = 1$. In addition to these geometric boundary conditions, an initial boundary condition is required for Eq. (14).

1. <u>Hydrodynamically Fully Developed Flow</u>. If the flow is hydrodynamically fully developed, then the velocity is independent of x and Eq. (13) becomes

$$\frac{\partial^2 u}{\partial r^2} + \frac{1}{r} \frac{\partial u}{\partial r} = \frac{1}{4} \frac{dp}{dx} = constant \qquad (21)$$

The integration of Eq. (21) with the boundary conditions defined by Eqs. (15) and (16) leads to Lamb's [20] fully developed velocity profile for the annulus as given below:

11

$$u = \frac{2}{M}\left(1 - r^2 + B \ln r\right) \qquad (22)$$

where

$$B = \frac{(r_2^2 - 1)}{\ln r_2}$$

and

$$M = 1 + r_2^2 - B.$$

2. <u>Flow in The Entrance Region</u>. The problem of laminar flow heat transfer in the entrance region was extensively studied during the past three decades. However, these studies were limited to some simple cases such as uniform heat flux, uniform wall temperature, and steady-state temperature distribution. For the current problem of a transient temperature distribution, none of the previous studies can be applied directly and therefore a re-examination is necessary.

To find the velocity distribution, an additional equation is required since there are three unknowns, u, v, and p, appearing in Eq. (12) and (13). The integral continuity equation is used.

$$\int_{r_2}^{1} ru\, dr = \frac{1 - r_2^2}{2} \qquad (23)$$

Because the momentum equation, Eq. (13), is nonlinear in u, it is difficult to solve by analytical methods. Instead, a direct numerical method is used to solve this problem.

To find the temperature distributions in the flowing fluid and the heat fluxes between the flowing fluid and the PCM, the energy equation must be solved. If the velocities and the boundary conditions for the energy equation are known, it is not difficult to solve the problem, however, if the boundary condition between the flowing fluid and the PCM is unknown, a technique of finding the boundary condition is needed.

IV. NUMERICAL PROCEDURE

A. VELOCITY PROFILES IN THE ENTRANCE REGION

Although some methods [17,18,19] were previously used to find the laminar velocity distribution of an annular passage in the entrance region, the previous methods are complicated and therefore are not very practical for this study. A much simpler method will be used.

By choosing an arbitrary value for p_j, then have only two unknowns, u and v. The procedure of finding u and v is: (1) give an arbitrary value for v (2) solve u by the Gaussian elimination method, (3) solve v by the Gaussian elimination method, (4) compare the new u with that in the previous iteration and if the difference is sufficiently small, then u and v obtained can be considered satisfy for the value of p_{j-1}, otherwise, using the new value of u and v and return to procedure (2).

Since u and v are obtained by choosing an arbitrary value for p_j, therefore u may or may not satisfy the integral continuity equation. An iterative solution for p_j is required and the value of p_j is considered to be converged if and only if

$$\left| \int_{r_2}^{1} ru\,dr - \frac{1 - r_2^2}{2} \right| \leq \epsilon \qquad (24)$$

where ϵ is the convergence criteria. The strategy to find p_j is that if the chosen value of p_j is smaller than the exact value, then

$$\int_{r_2}^{1} ru\,dr < \frac{1 - r_2^2}{2},$$

14

and a larger value of p_j is used in next iteration. The Newton-Raphson method is used to find p_j.

B. ITERATIVE SOLUTION OF THE INNER-WALL TUBE TEMPERATURE

Since the enthalpy equation nor the energy equation can be used without giving the temperature distribution between the heat transfer fluid and the PCM, the iterative solution of the inner tube wall temperature, T_1, becomes a starting procedure for the calculation of the heat transfer in the latent thermal storage system. Since this temperature is between the inlet fluid temperature and the initial PCM temperature, the iterative solution converges.

C. SOLVING THE MELTING/FREEZING PROBLEM

The boundary conditions of Eq.(9) are given by:

$$\phi \Big|_{r=r_1} = \frac{\rho C_p (T_1 - T_f)}{\lambda} \qquad (25)$$

$$\frac{\partial \phi}{\partial r} \Big|_{r=0} = 0 \qquad (26)$$

$$\frac{\partial \phi}{\partial \chi} \Big|_{\chi=0} = \frac{\partial \phi}{\partial \chi} \Big|_{\chi=L} = 0 \qquad (27)$$

Equation (27) is based on the assumption that the two end-plates for the PCM tube have very low thermal conductivities so that they are considered to be adiabatic.

15

The enthalpy distribution in the PCM at a fixed axial location can be easily obtained by using Eq. (10) and the appropriate boundary conditions. The temperature distribution is obtained from Eq. (11). The new θ from the last time step is a result of radial conduction and axial conduction during the time step. The θ obtained from Eq. (10) is not appropriate to be used for the calculation of the heat flux between the heat transfer fluid and the PCM. The equation which resembles Eq. (10) but lacks the axial conduction term is given below and is used for the purpose of calculating the heat flow.

$$\frac{\tilde{\theta}_{i,j}^{m+1} - \theta_{i,j}^m}{\Delta \tau} = \frac{2}{r_{i+1} + r_i} \frac{[(\phi_{i+1,j}^m - \phi_{i,j}^m)\,r_{i+1} - (\phi_{i,j}^m - \phi_{i-1,j}^m)\,r_i]}{\Delta r^2} \qquad (28)$$

where

$$\tilde{\theta} = \frac{2}{\rho\,(r'^2_{i+1} - r'^2_i)\,\Delta x'} \int_0^V \rho\,\frac{(i - i_i^*)}{\lambda}\,dv$$

The transient local heat flow rate for a length of $\Delta x'$ at $r = r_1$ is given by

$$q(t, x') = \frac{\sum V_i\,\rho_p\,\lambda\,(\tilde{\theta}_i^{m+1} - \theta_i^m)}{\Delta t'} \qquad (29)$$

where

$$V_i = \pi(\,r'^2_{i+1} - r'^2_i)\,r_1^2\,\Delta x'$$

and

$$\Delta t' = \frac{\Delta\tau \, r'^2_1}{\alpha_p}.$$

Therefore the transient local heat flow per unit length is given by

$$Q_{x1}(t, x') = \frac{q(t, x')}{\Delta x'} \qquad (30)$$

D. TRANSIENT TEMPERATURE DISTRIBUTION OF THE HEAT TRANSFER FLUID

From the integration of the one-dimensional heat conduction equation for cylindrical coordinates with the boundary conditions where

$$T = T_1 \qquad \text{at} \qquad r' = r'_1$$

and

$$T = T_2 \qquad \text{at} \qquad r' = r'_2$$

and using Fourier's law, one has

$$Q = \frac{2\pi k_t (T_2 - T_1)}{\ln(r'_2/r'_1)} \qquad (31)$$

where Q is the heat flow rate through the PCM tube per unit length.

Equation (31) is obtained based on the assumptions that the tube wall is very thin so that the axial conduction and the sensible heat absorbed by the tube are neglected.

17

Since the heat flow through the PCM tube is equal to the heat flow from the PCM tube to the PCM, from Eqs. (30) and (31) one has

$$T_2(t, x') = \frac{Q_{x1}(t, x') \cdot \ln(r'_2/r'_1)}{2\pi k_t} + T_1(t, x') \tag{32}$$

Upon finding the temperature distribution of the HTF, the Nusselt numbers can then be calculated. According to Fourier's law, the local heat flow per unit length between the heat transfer fluid and the PCM can be given by

$$Q_{x2}(t, x') = 2\pi r'_2 k_h \frac{\partial T}{\partial r'}\Big|_{r'=r'_2} \tag{33}$$

The bulk temperature of the heat transfer fluid is

$$T_b = \frac{\displaystyle\int_{r_2}^1 uTr\,dr}{\displaystyle\int_{r_2}^1 ur\,dr} \tag{34}$$

By definition, the Nusselt number is

$$Nu = \frac{h\,D_h}{k_h} = \frac{2h(r'_o - r'_2)}{k_h} \tag{35}$$

The heat flux by conduction at the outer PCM tube surface is equal to the heat flux by convection to the HTF. Thus,

$$h(T_b - T_2) = k_h \frac{\partial T}{\partial r'}\Big|_{r'=r'_2} \tag{36}$$

The combination of Eq. (40) and Eq. (41) yields

18

$$Nu = \frac{2(1 - r_2)}{T_b - T_2} \left. \frac{\partial T}{\partial r} \right|_{r=r_2} \tag{37}$$

It is remembered that all the values concerning the heat transfer between the heat transfer fluid and the PCM and the values concerning the melting/freezing in the PCM are based on the iterative T'_1 and it may not be converged. T'_1 is considered to be converged if and only if

$$|Q_{x1} - Q_{x2}| \leq \epsilon \tag{38}$$

where ϵ is the convergence criteria. If T'_1 is not converged, then one has to correct it and return to the solution procedure described of solving the melting/freezing problem. This is a root finding problem and T'_1 is found by the Newton-Raphson method.

V. EXPERIMENT

The experimental apparatus employed in this study is shown schematically in Fig. 3. The experimental setup consists of three systems: the instrumented heat exchanger system, the fluid flow control system, and the data acquisition system. The instrumented heat exchanger system consists of a video camera, a paddlewheel flow meter, controllable light source, and a latent thermal storage unit. The video camera is accompanied by a video cassette recorder (VCR) for photographic data recording. Specifications for the video camera are provided in Table 1. The paddlewheel flosensor is accompanied by a digital meter for heat transfer fluid flow rate monitoring.

Table 1.   VIDEO CAMERA SPECIFICATIONS

Unit	Panasonic WV-3250/8AF color video camera
Specification (lens)	
Auto focus	
Zoom ratio	8x
Focal length	10.5 - 84 mm
Max. apeture ratio	1:1.4 (F1.4)
Macro range	5 cm - 1.3 m
White balance	Auto tracing white balance or manual setting

The shell and tube heat exchanger consists of a 3 in. (7.62 cm) inner diameter shell around a removeable cartridge of tubes. Each cartridge consists of eight capped tubes filled with PCM and two support disks. The disks were designed to provide four functions, which are: provide a support frame for the tube bundle, align fluid flow over the tubes, align thermocouples and form a plenum region between the cartridge and the end plates of the shell. The plenum regions serve to maintain a full level of fluid flow over the PCM containment tubes. Both the shell and cartridge were fabricated from Lexan. Lexan is a transparent polycarbonate, thereby enabling visual access to the phase change phenomena. As a heat transfer material Lexan suffers from low thermal conducitvity, but the limiting heat transfer resistance in this shell and tube heat

Figure 3. Experimental Apparatus

COOLER

BATH CIRCULATOR

REMOTE SENSOR

TEMP. PROGRAMMER

FLUID FLOW CONTROL SYSTEM

VALVE

LIGHT

LATENT THERMAL ENERGY STORAGE UNIT

PADDLEWHEEL FLOWMETER

INSTRUMENTED HEAT EXCHANGER SYSTEM

VIDEO CAMERA

COLOR MONITOR

VCR

MICROCOMPUTER

KEYBOARD

THERMOCOUPLE ANALOG BOX

DIGITAL FLOWMETER

DATA ACQUISITION SYSTEM
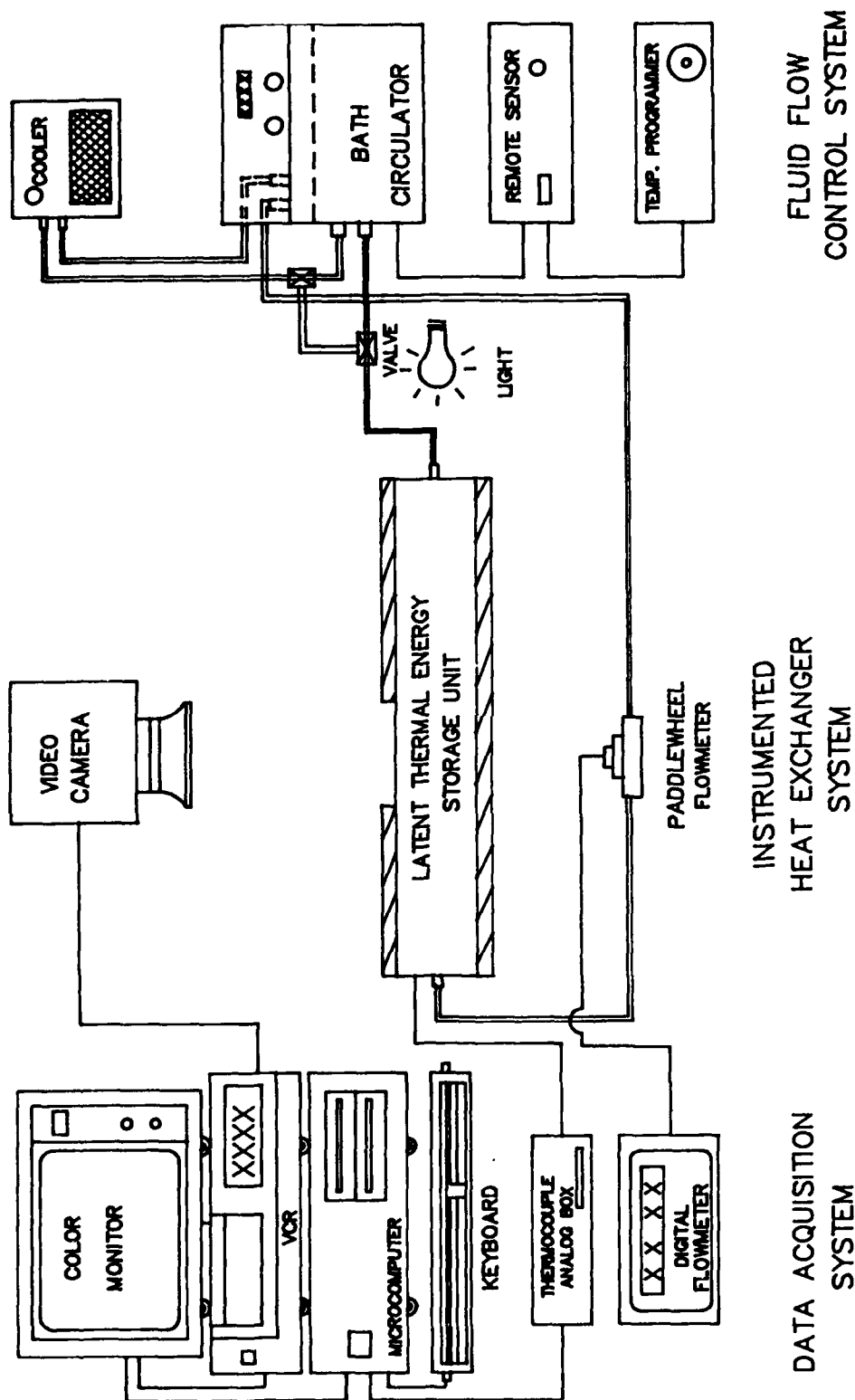
exchanger was determined to be the PCM. Therefore for experimental purposes Lexan was an excellent choice. The heat exchanger is sealed with end plates that are grooved for a gasket to prevent leakage. These end plates have holes tapped for the inlet and outlet fluid flow ports, and also for the thermocouple fittings. A total of four copper-constantan subminiature thermocouples were fitted in the inlet and outlet positions of the cartridge. Another copper-constantan thermocouple was fabricated and placed inside one of the PCM containment tubes approximately halfway between the inlet and outlet for PCM temperature monitoring.

A second shell and tube heat exchanger, utilizing the same shell from the first heat exchanger, was designed to improve photographic capabilities. A single 2 in. (5.08 cm) diameter PCM containment tube was fabricated out of Lexan, with a thermocouple fitting located at the front end of the tube. A copper-constantan thermocouple was used to monitor the PCM temperature, at an axial distance from the inlet of the PCM tube of 8.4 in. (21.34 cm). Incorporated into the design was a higher outlet fluid flow port to facilitate the purging of the initial air inside the storage unit. Table 2 lists the specifications of both heat exchanger configurations; the tube bundle and the single containment tube.

Table 2. SHELL AND TUBE HEAT EXCHANGER SPECIFICATIONS

Parameter	Tube Bundle	Single Tube
Shell Inner Diameter (cm)	7.62	7.62
Shell Wall Thickness (cm)	0.47	0.47
Tube Outer Diameter (cm)	0.953	5.08
Tube Inner Diameter (cm)	0.635	4.76
Material	Lexan	Lexan
Conductivity (W/mC)	7.96	7.96
Total PCM Volume (cm3)	15.6	882.0
Flow Length (cm)	49.2	49.5

The fluid flow control system consists of a fin and tube air cooled heat exchanger (cooler), a constant temperature both circulator, an electronic temperature programmer, and a remote sensor. The bath/circulator incorporates a dual pump, a heater, and a sensor into a fluid reservoir. An electronic controller is mounted on top of the reservoir. The cooler is used in conjunction with the bath/circulator during the freezing process. The cooler is also used in the temperature programmer is a linear programmmer which is connected to the bath/circulator via the remote sensor. The programmer can accurately control the temperature of the heat transfer fluid. Table 3 gives the details of the fluid flow control system.

Table 3.   FLUID FLOW CONTROL SYSTEM SPECIFICATIONS

Constant Temperature Bath Circulator:
   Unit   Neslab EX-100DD
   Specifications
      Range   Ambient to 266 F (130 C)
      Stability   0.018 F (0.01 C)
      Max Pumping   3.35 gpm (13 l/min)
      Heater   800 Watts

Fin and Tube Air Cooler Heat Exchanger (Cooler):
   Unit   Neslab Aerocool 100
   Specifications
      Lower limit   3.6 F (2 C) above ambient
      Fan speed   adjustable

Remote Sensor:
   Unit   Neslab RS-1
   Specifications
      Sensor   Platinum RTD
      Resolution   0.18 F (0.1 C)

Electronic Temperature Programmer:
   Unit   Neslab ETP-3
   Specifications
      Programming   Linear
      Time Interval   10-10,000 minutes
      Clock Pulse   100 microseconds

The data acquisition system is a microcomputer based data logger. This system consists of an IBM PC/XT with a Strawberry Tree Analog Connection System

installed, a high resolution color monitor, a high quality (HQ) VCR, and a digital fluid flowmeter.

The Strawberry Tree Analog Connection has a menu driven data acquisition program which also has process control capabilities. Connections for the thermocouples and for the signal conditioner of the flowmeter are provided by an analog to digital (A/D) terminal box. The terminal box provides input channels to the microcomputer for on-screen flow rate and temperature monitoring and floppy disk recording. The monitor has dual capability as a high resolution, digital RGB input monitor and as a color display for the VCR. The HQ VCR is used to monitor, record and replay the photographic image of the solid-liquid phase front motion. The VCR has a slow speed replay feature for frame-by-frame advance of the type. The VCR recording can be still framed and the resulting picture photographed by a 35mm camera. The digital fluid flowmeter converts the frequency signal from the paddlewheel flosensor to a four digit display of the volumetric flow rate. Table 4 gives the details of the data acquisition system.

Table 4.   DATA ACQUISITION SYSTEM SPECIFICATIONS

Microcomputer based Data Logger:

Unit	IBM PC/XT with Strawberry Tree Analog Connection System
Specifications	
No. of Channels	8
Resolution	0.015%
Accuracy	0.04%
Read rate	0.3 to 5 msec

Video Cassette Recorder:

Unit	Toshiba M-2400 VHS video cassette recorder

35mm Camera & Lens:

Camera	Minolta Advanced Maxxum 7000 35 mm SLR camera
Lens	Minolta Maxxum 70-210 mm f/4.0 with macro zoom

The video camera and VCR were employed in the experiments because of unsuccessful attempt to use a Micorneye Bullet digital imaging system to track the phase front progression. Attempts were made to improve the digital image that was received from the system. Modifications to the background lighting, focal lenght of the lens, and the apeture of the lens were made. However these modifications could not overcome the depth of field limitaions of the Microneye Bullet system when viewing the curved surfaces of the PCM containment tubes. The depth of field of the Microneye camera was less than 1 cm, which was too small to obtain an accurate image. Table 5 is a comparision between the Microneye digital imaging system and the VCR/video camera setup used in the experiments. The video camera provides a greater depth of field and faster iris control when compared to the Microneye camera, and this led to a much improved image of the PCM phase front.

A. TEST MATERIALS

The phase change materials were selected based on their availability and melting temperature. Low melting temperature materials were selected because of their application in Spacecragr Thermal Management Systems. Importance was also placed on materials that would allow clear visual indentification of the phase change front motion.

P116, a Sun wax, was selected as a PCM to be tested. P116 is a paraffin which is clear as a liquid but opaque as a solid. Melting occurs with limited segregation of components and upon freezing P116 tends to pull away from it's container, which has an apperciable effect on heat transfer. Also, paraffin waxes display little supercooling.

E-1000, a polyethylene glycol, is a stable organic polymer. E-1000 displays no supercooling and is compatible with many materials. E-1000 is white as a solid and transparent as a liquid.

C-31 is a cross-linked polymer formulation of $Na_2SO_4 - 10H_2O$. The phase change process is not the traditional freeze/melt concept but a solid transition. Therefore, there is no phase change driven separation or stratification. Properties for the test materials may be found in Table 6.

Water was selected as the heat transfer fluid. It is clear, abundantly available, and inexpensive. It is used in a variety of thermal storage and heat transfer related applications. Also water is transparent and thereby does not interfere with the viewing of the phase change phenomena.

Table 5.   COMPARISION OF IMAGING TECHNIQUES

Characteristic	Imaging Technique	
	VCR/Video Camera	Digital Imaging (Microneye)
Frames/sec	30	15
Resolution	325 lines	128 x 256
Color	Color	4 Gray tones
RS-170 Output	Yes	No
Depth of Field (Max)	8.4 cm	< 1 cm
Format	VHS - 1/2 in.	
Iris Control	Fast	Slow
Labeling	Clock/Text	N/A
Cost	Moderate	Low

Table 6.   PROPERTIES OF THE TEST MATERIALS

PROPERTIES	PCM		
	P116	C-31	E-1000
Melting Point (C)	43.0	31.0	38.0
Heat of Fusion (KJ/Kg)	226	200	172
Specific Heat (KJ/KgC)	2.75	2.09	2.05
Conductivity (W/mC)	0.24	0.61	
Density—Solid (Kg/m3)	818	1420	1123
Density—Liquid (Kg/m3)	760		

VI. EXPERIMENTS

A. DIFFERENTIAL SCANNING CALORIMETRY

Differential scanning Calorimetry (DSC) tests were performed on p116 to verify melting and recrystallization temperatures, and the latent heat of fusion value. A Perkin-Elmer DSC-4 Differential Scanning Calorimeter and a Perkin-Elmer Model 3600 Data Station erer employed to perform the tests. Figures 4 and 5 represent the results of these tests.

DSC tests were also performed on C-31. However, difficulties were encountered. C-31 is a polymer formulation of a salt hydrate and during the tests the water would be driven off, therefore giving ficitious results of the test sample energy output. Mechanical sealing ot the sample containers was ineffective in preventing this phenomena. Chemical bonding of the sample containers was also ineffective.

B. P116 SUN WAX

P116, a Sun wax, was tested using two different heat exchanger assemblies. A cartridge design and a single containment tube exchanger was used.

1. Tube Bundle Results. Experiments were performed for both the melting and freezing of the PCM. In each case two trials were completed at each of two flow rates: 0.6 gpm (2.27 l/min) and 1.22 gpm (4.62 l/min).

For the melting process, data acquisition began once thermal equilibrium in the heat exchanger was extablished at a temperature below the melting point of the PCM. The setpoint of the constant temperature bath was set at 48 C and inlet, outlet and PCM temperature were recorded until melting was complete. For the freezing process, data acquisition began once the setpoint of the constant temperature bath was set at
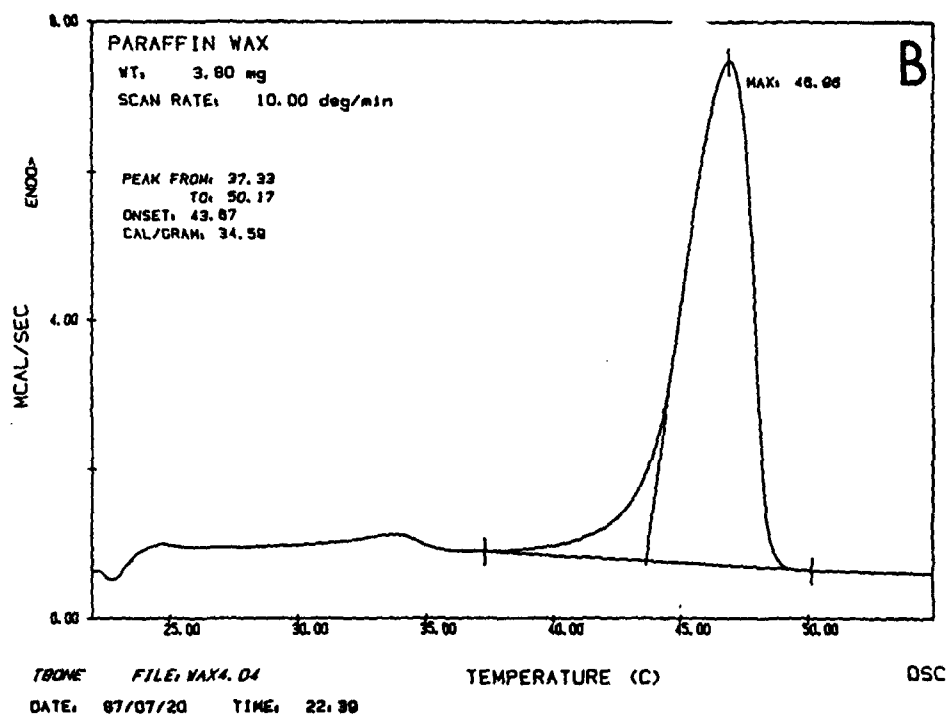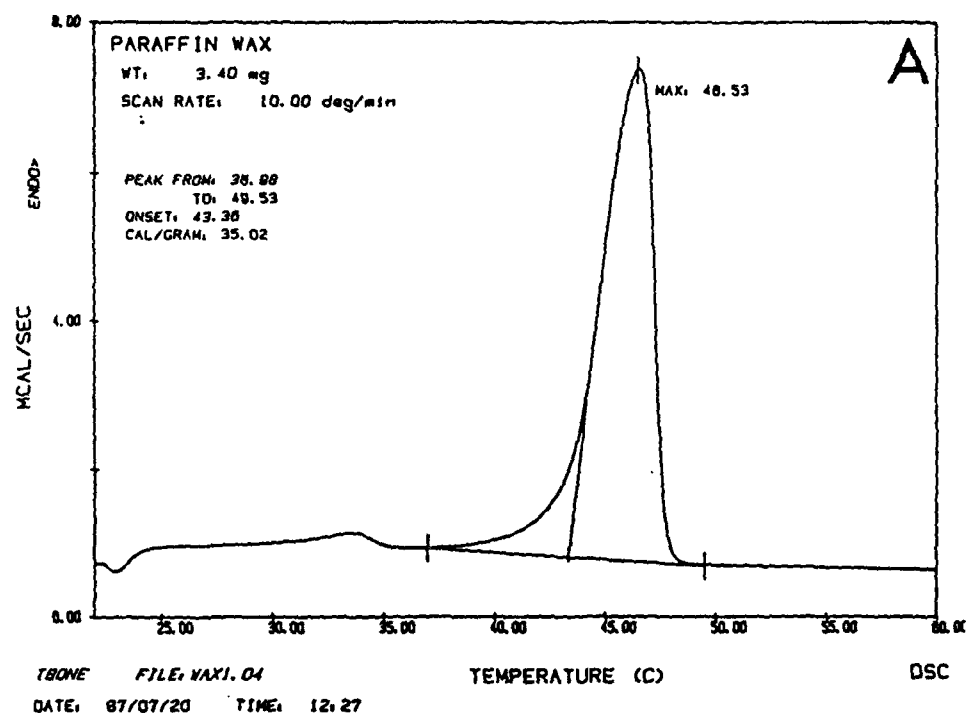
Figure 4. DSC Results for Melting of P116: (A) h = 147.33 KJ/KG, (B) h = 144.78 KJ/KG

A

PARAFFIN WAX
WT: 2.90 mg
SCAN RATE: 1.00 deg/min

PEAK FROM: 35
TO: 47.47
ONSET: 42.92
CAL/GRAM: 36.88

MAX: 44.89

ENDO>

MCAL/SEC

1.00

0.50

0.00

25.00   30.00   35.00   40.00   45.00   50.00

TBONE   FILE: WAXB.D4   TEMPERATURE (C)   DSC
DATE: 87/07/22   TIME: 10:55

B

PARAFFIN WAX
WT: 3.80 mg
SCAN RATE: -10.00 deg/min

PEAK FROM: 33.87
TO: 44.77
ONSET: 42.96
CAL/GRAM: -34.18

MIN: 41.84

ENDO>

MCAL/SEC

8.00

4.00

0.00

25.00   30.00   35.00   40.00   45.00   50.00

TBONE   FILE: WAXS.D4   TEMPERATURE (C)   DSC
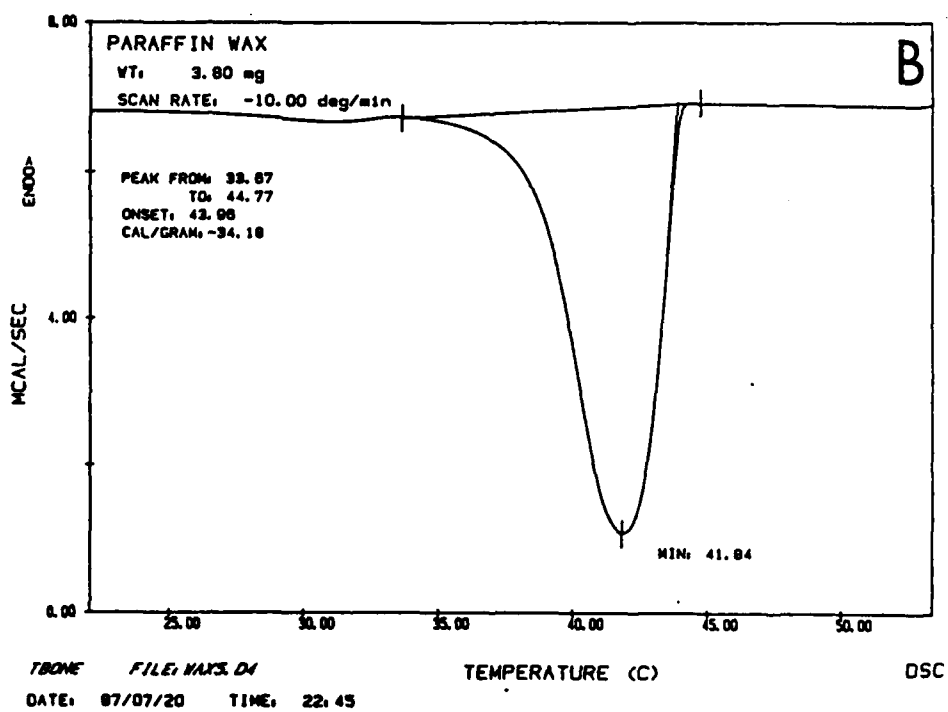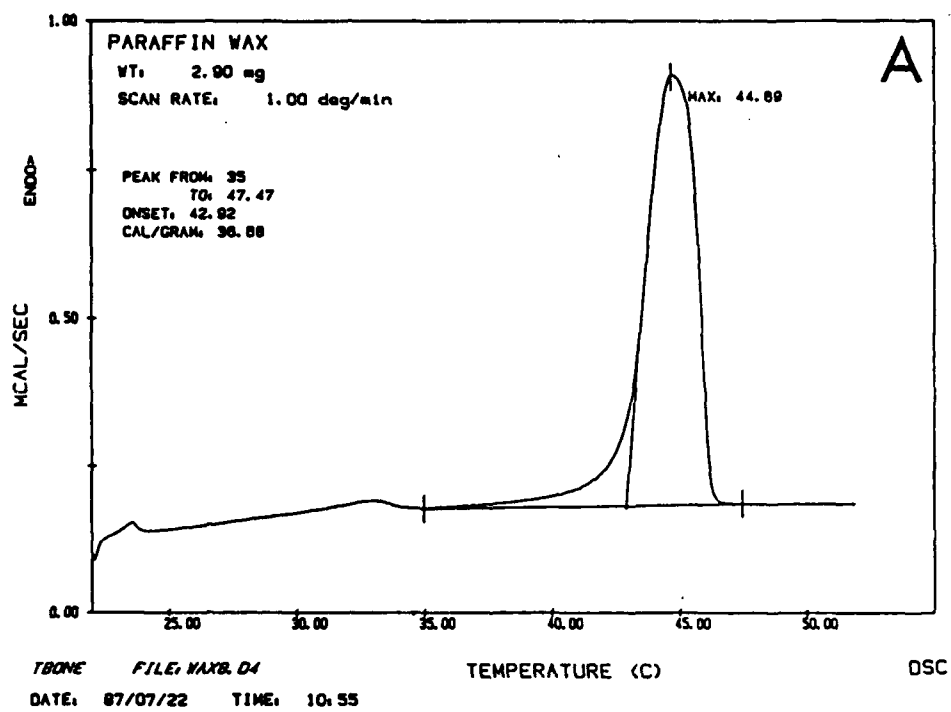DATE: 87/07/20   TIME: 22:45

Figure 5.   DSC Results for Melting (A) and Freezing (B) of P116

43 C, the air cooler was turned on, and data acquisition was continued until freezing was complete.

Figures 6-9 represent on selected trial for each experimental condition. The inlet temperature repersents the temperature of a single Thermocouple located at the beginning of the PCM tubes. The PCM temperature represents the temperature of one of the two thercocouples located interstitially in the PCM. The outlet temperature is the temperature of one of the three thermocouples located at the end of the PCM tubes. This method of data reduction was chosen because of the lack of data scatter between trials and also due to the lack of data scatter between thermocouples in the outlet and PCM for each trial. As a measure of repeatability, heating and cooling rates of the PCM for each trial were calculated. For the low flow rate, heating rates of 0.28 C/min and 0.74 C/min, and cooling rates of 0.44 C/min were found. Comparable results were obtained for the high flow rate. Reynolds and Stefan numbers were calculated in all experiments as follows:

$$Re = V D_h \rho / u \text{ and } Ste = c_p \Delta T / h$$

where v is the velocity of the heat transfer fluid, D_h is the hydraulic diameter, ρ is the density of the HTF, μ is the viscosity of the HTF, c_p is the average specific heat of the PCM, ΔT is the temperature swing of the PCM, and h is the latent heat of fusion. The temperature swing of the PCM in this case would be the difference of the final PCM temperature and the initial PCM temperature.
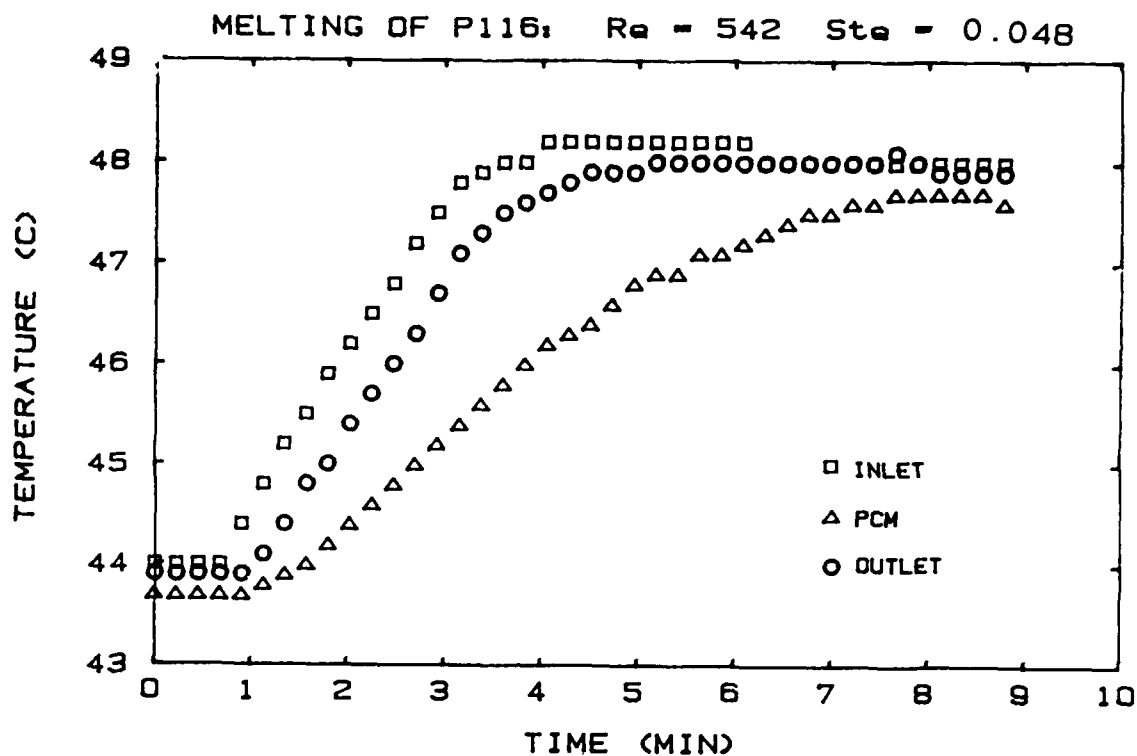
Figure 6.   Experimental Temperatures for Melting of P116, 0.6 gpm (2.271 l/min)
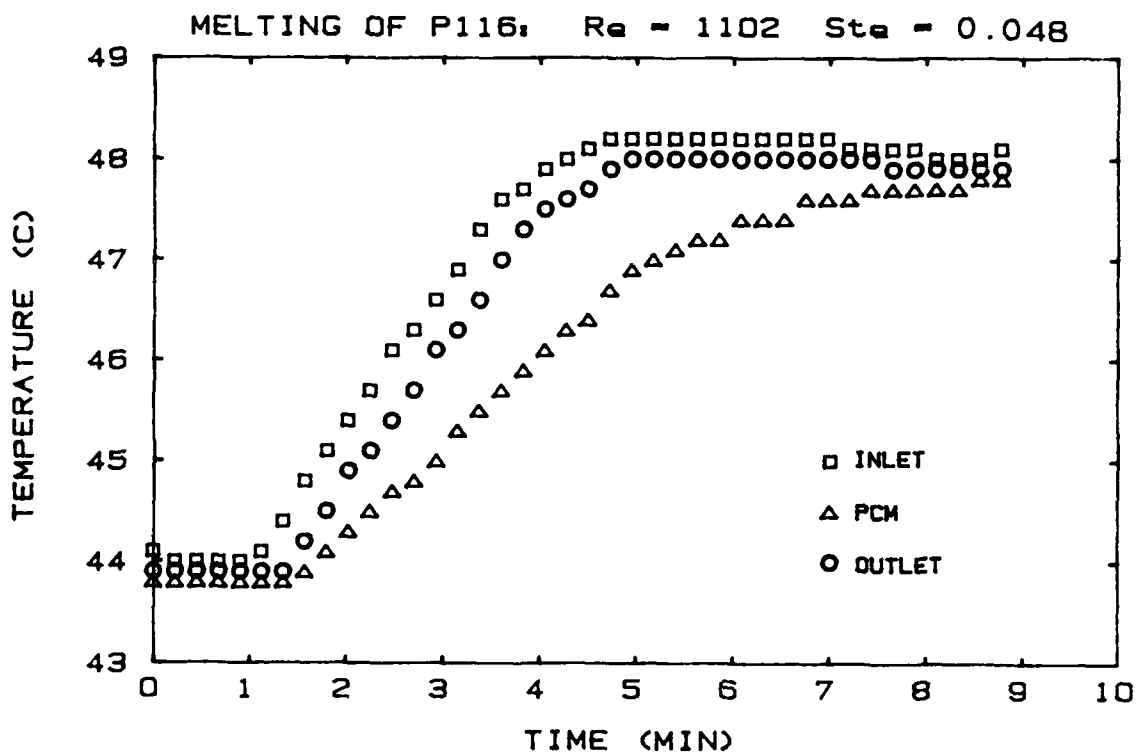

Figure 7.   Experimental Temperature for Melting of P116, 1.22 gpm (4.62 l/min)
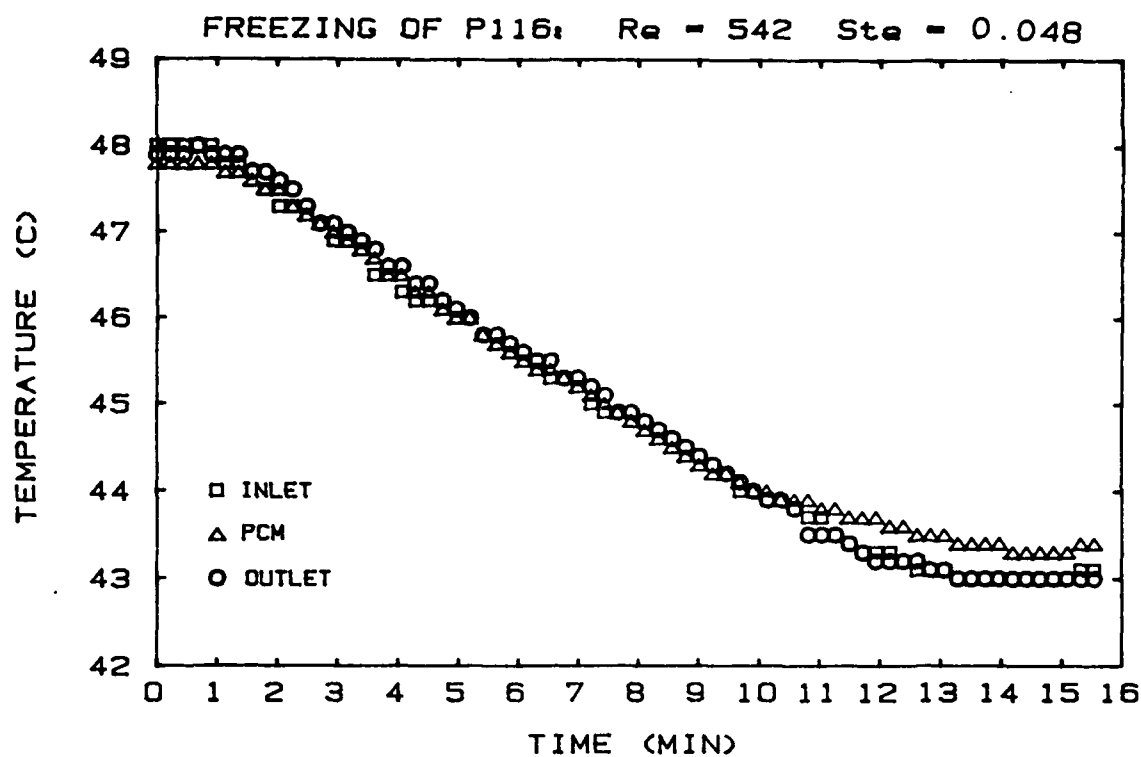
FREEZING OF P116:   Re = 542   Ste = 0.048

Figure 8.   Experimental Temperature for Freezing of P116, 0.6 gpm (2.27 l/min)

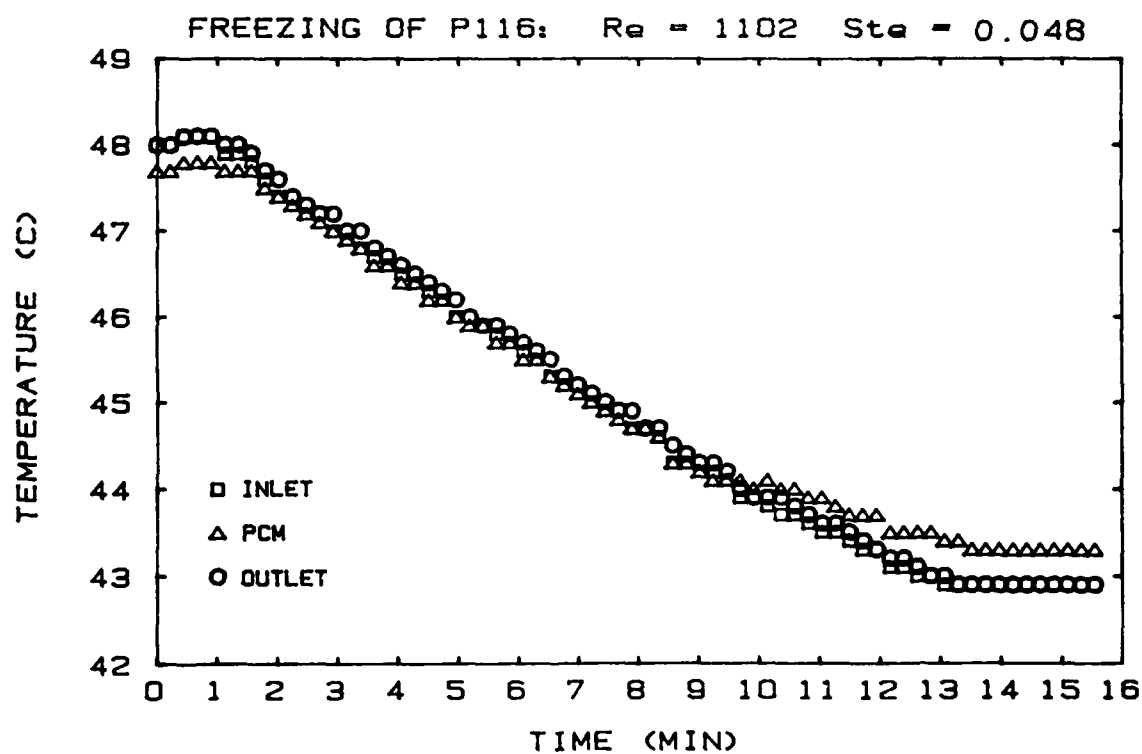FREEZING OF P116:   Re = 1102   Ste = 0.048

Figure 9.   Experimental Temperature for Freezing of P116, 1.22 gpm (4.62 l/min)

34

Figures 6 and 7 represent selected results for the melting process for the low and high flow rates respectively. The PCM temperature was not constant during melting. This is most likely due to the non-uniformity of P116. The inlet temperature is shown to overshoot the constant temperature bath setpoint of 48 C, as the bath compensates for the thermal inertial of the heat exchanger. Figures 8 and 9 represent selected results for the freezing process for the low and high flow rates respectively. The inlet temperature decreases linearly without overshooting the bath setpoint of 43 C. The heater in the constant temperature bath and the air cooler work together to decrease the temperature without overshooting the setpoint. It is important to note that the air cooler is not a refrigeration unit and that the maximum amount of cooling was provided during the freezing experiments.

The video camera provided a qualitative insight to the nature of melting and freezing of P116. P116 wax is clear as a liquid but opaque as a solid, thus enabling visual identification of the phase front. For each trial, the video camera and VCR were used to tape the entire experiment. At the low flow rate, visulaization was limited dure to air bubbles adfering to the outside of the PCM tubes. Air bubbles were not a problem at the high flow rate as melting progressed non-uniformly in the video. Observation of the freezing process, however, was limited due to the initial frosting of the inside PCM tube walls at the onset of freezing.

2. <u>Single Tube Results</u>. An experiment was performed for the melting of P116 in a single containment tube at a flow rate of 0.65 gpm (2.95 l/m). Thermal equilibrium was established in the heat exchanger at a temperature of 39 C. Flow was shut off to the heat exchanger. Once the bath temperature reached 49 C, fluid flow was initiated into the heat storage unit and the data acquisition process was begun and continued unitl melting was complete. During the experiment, the inlet temperature was held constant at 49 C. Figure 10 represents one test for the melting of P116 in the single

tube. The inlet, outlet and PCM temperatures are that of single thermocouples. A discontinuity in time of the PCM temperature is evident. This represents the phase change transition. Figure 11 and 12 are a succession of photographs of the phase change process for P116 was in a single tube. In each photograph the time is displayed. The thermocouple is visible and it acts to hold the solid PCM from falling to the bottom of the tube. The other photographs display the lowerhalf of the PCM tube. The time displayed on the photographs is consistent with the time displayed on the x-axis of Fig. 10. Additional tests for P116 were not performed due to the tube failure
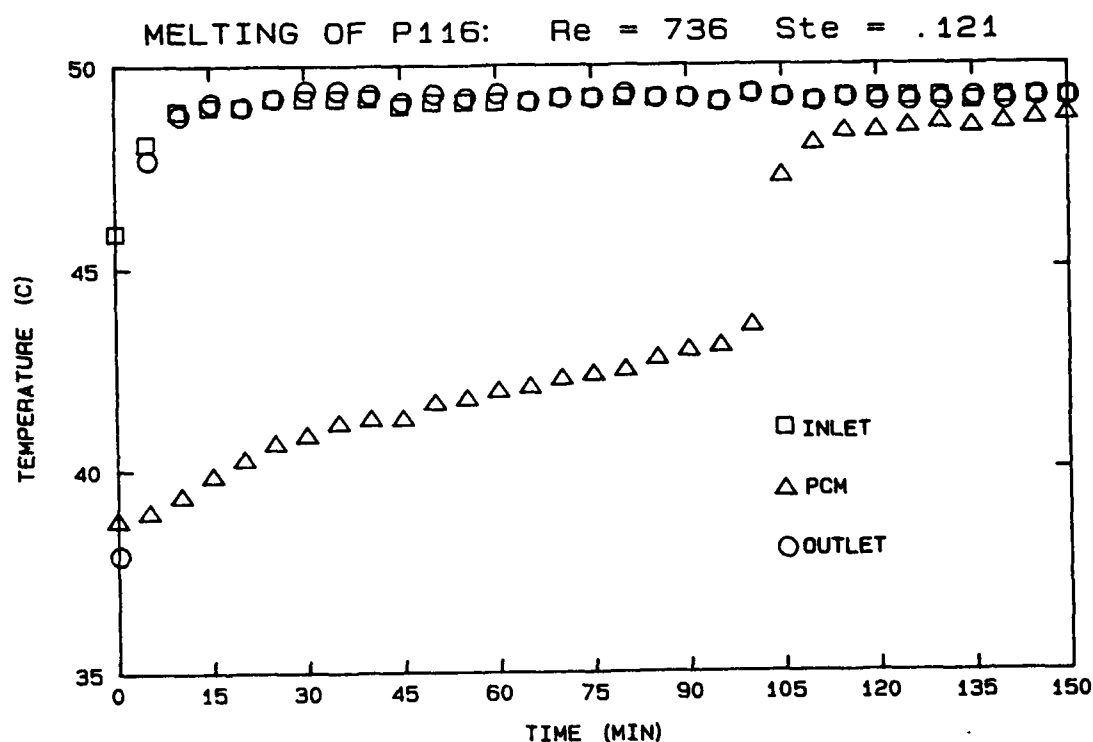

Figure 10. Experimental Temperature for Melting of P116, 0.65 gpm (2.46 l/min)
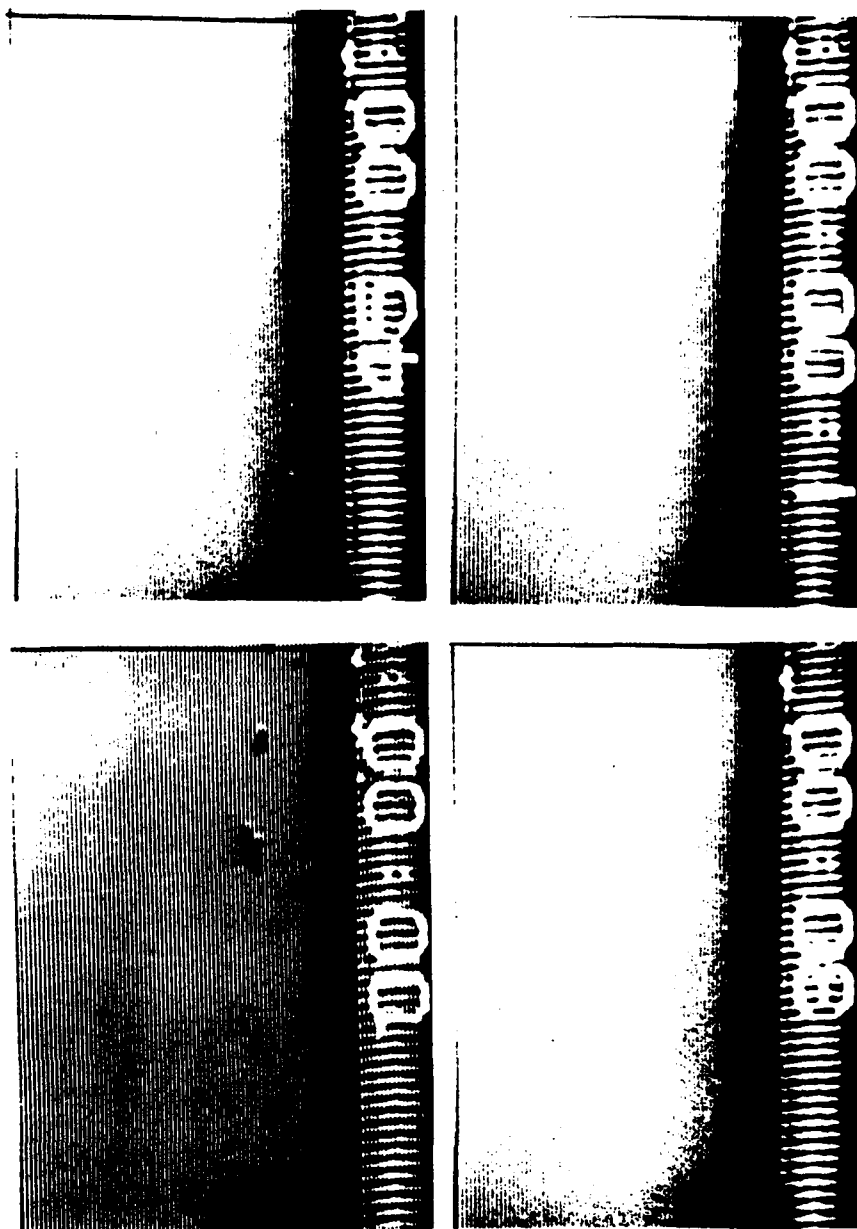
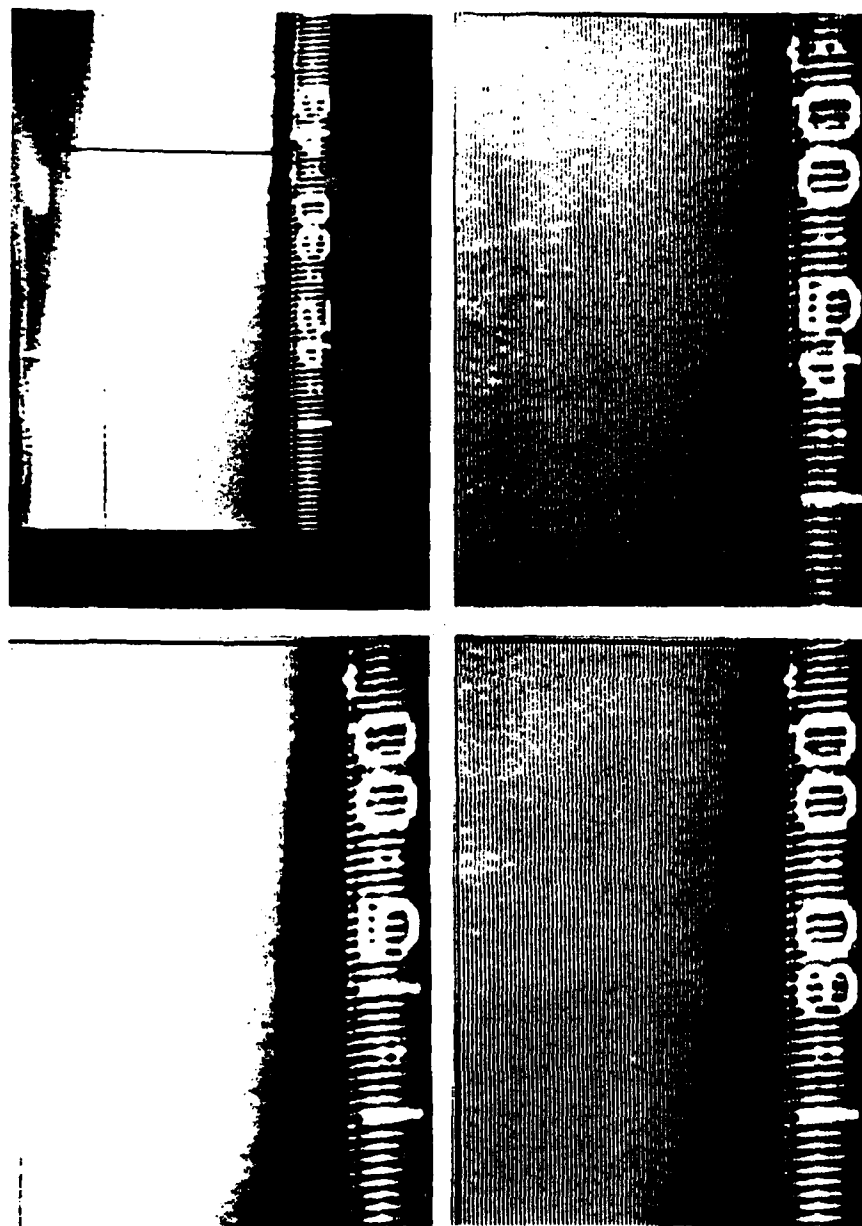Figure 11. Experimental Photographs for Melting of P116, 0.65 gpm (2.46 l/min)

Figure 12. Experimental Photographs for Melting of P116, 0.65 gpm (2.46 l/min)

C. CALOTHERM C-31

Experiments were performed for the melting of C-31 in the single containment tube at a flow rate of 0.3 gpm (1.34 l/min). Thermal equilibrium was extablished in the heat exchanger at a temperature of 30 C. Fluid flow was shut off to the heat exchanger. Once the bath temperature reached 55 C, fluid flow was initiated into the heat exchanger and the data acquisition process was begun and continued until melting was complete. When the experiment was in progress, the inlet temperature was held constant at 55 C.

Figure 13 displays two selected trials of the experiments performed on C-31. The inlet, outlet and PCM temperatures represent the temperature of single thermocouples. The PCM temperature increase gradually, and no sharp melting point transition is noticed. This is a result of the fact that phase change is actually a solid-solid transition. The top photograph in Fig. 14 displays stress cracks in the Lexan of the single containment tube that were presummably induced by the volume change of C-31. The damaging volume change was not expected since the phase change is a solid transition.

D. E-1000

Attempts were made to experiment with E-1000 contained in the eight cylindrical tubes of the cartridge design. Upon one melting-freezing cycle, tube failure occurred. Besides the leaking of was, volume change with phase change induced stress was evident. The bottom photograph in Fig. 18 displays the stress cracks.
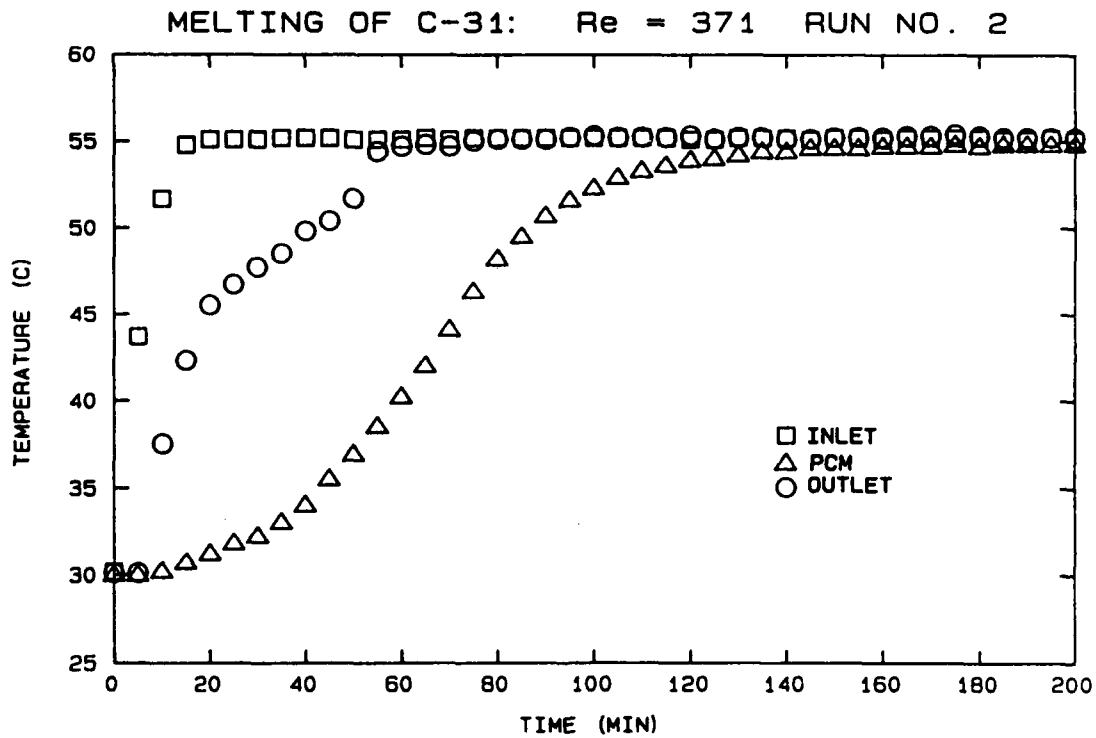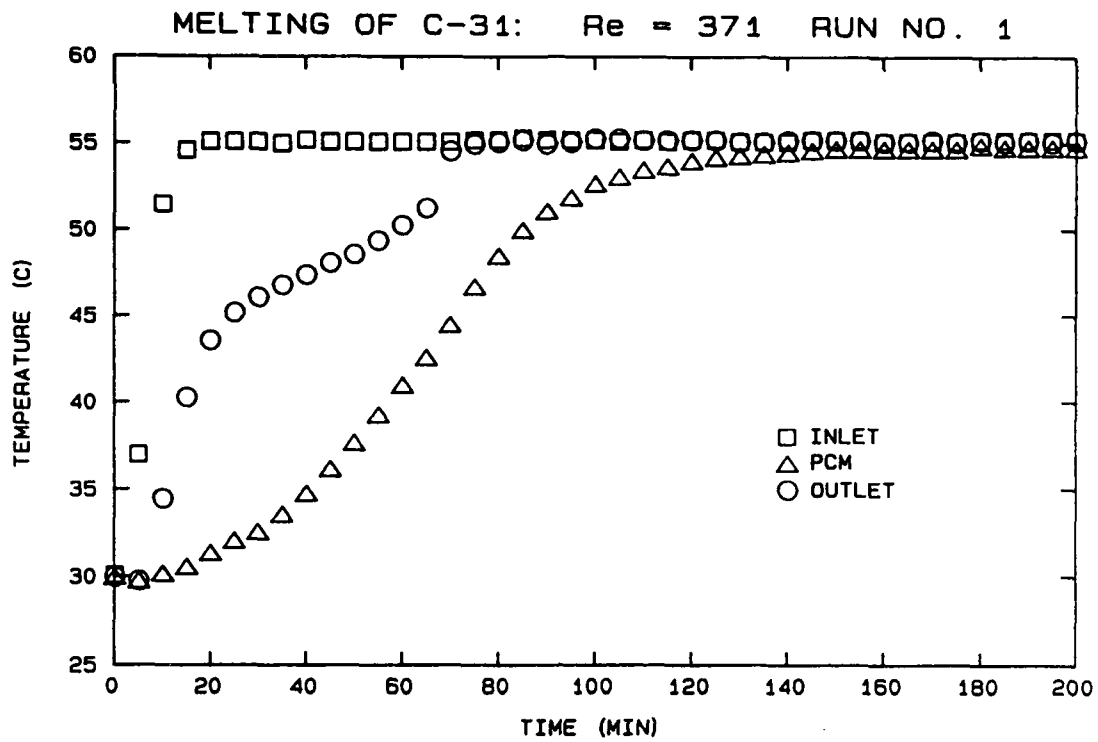
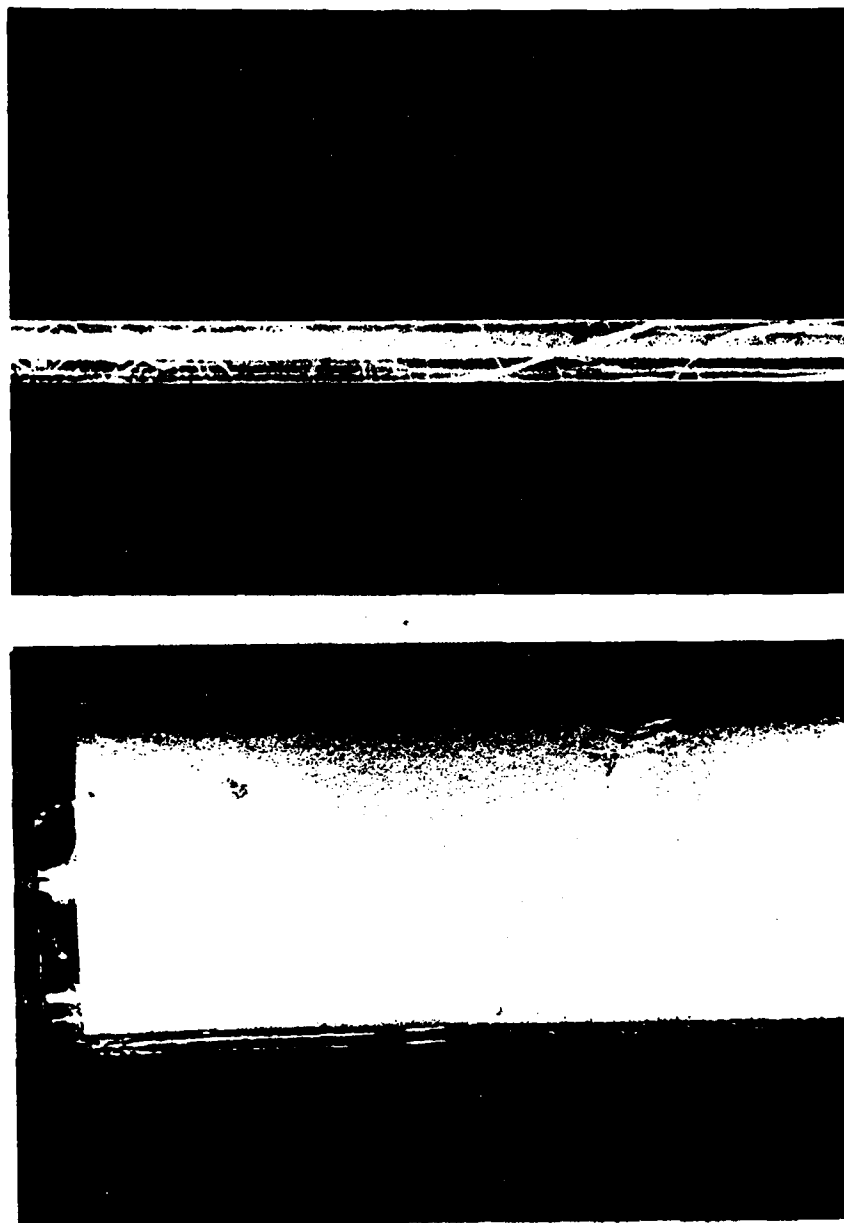Figure 13. Experimental Temperatures for Melting of C-31, 0.3 gpm (1.14 l/min)

Figure 14. Photographs of Stress Cracks on Lexan Tubes

VII. VERIFICATION OF ACCURACY

Since in recent studies many of the methods used are either new or improved from other methods, a comparison of the recent numerical results with experimental results or the results obtained by others is very important. This not only avoids mistakes made in recent studies but also provides an examination of the accuracy of recent methods.

We found that many of the previous studies were restricted to limited boundary conditions or simpler cases, therefore the comparisons with previous works are quite limited.

A. MELTING/FREEZING OF PCM IN A HORIZONTAL TUBE.

A comparison of the experimental data of Viskanta [22] and the predictions by the enthalpy method with n-heptadecane as the PCM, given in Fig. 15, shows quite good agreement. In Fig. 15 the Stefan number, Ste, and the initial dimensionless temperature, ϕ_{ini}, are defined as:

$$Ste = \frac{c_p(T_f - T_1)}{\lambda} \tag{39}$$

$$\phi_{ini} = \frac{T - T_1}{T_f - T_1} \tag{40}$$

B. ENTRANCE REGION VELOCITY DISTRIBUTION

The method used in this investigation to find the laminar velocity distribution in the entrance region of an annulus is very simple when compared with the eigenvalue method. When computing on IBM 4381 system for 41 x 501 grids, the CPU time is only 86 seconds. The comparison of maximum velocity distribution by Heator et al.
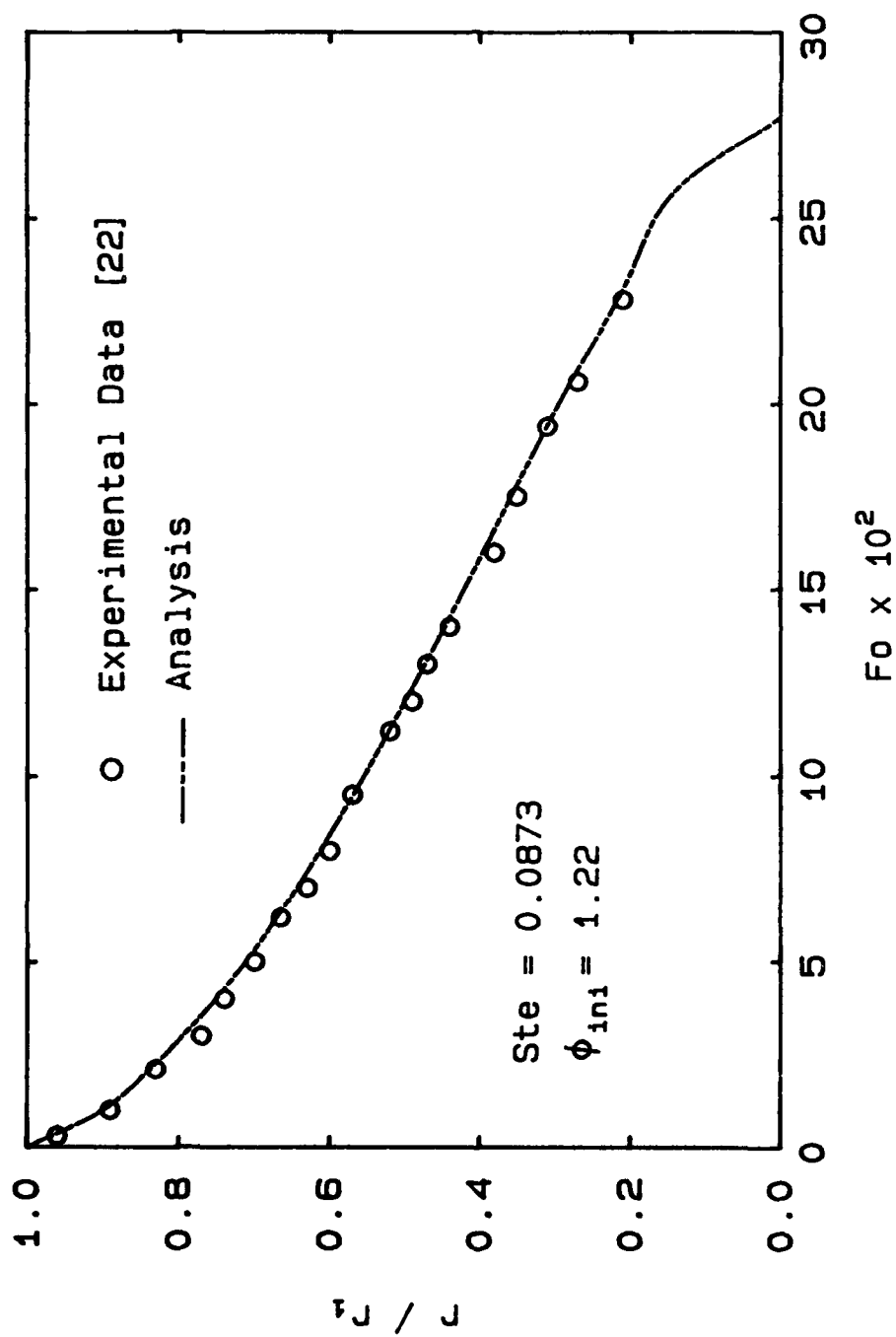
Figure 15. Comparison of predicted solid-liquid interface position with data for solidification of n-heptadecane

[19] and this work is given in Fig. 16. When the flow is fully developed, the velocity profile obtained by this method has a maximum difference of only 0.02% compared with Eq. (22) for the case of $r_2 = 0.5$ and 11 grid points in the radial direction. A comparison of the fully developed velocity profiles obtained from Eq. (22) and from the numerical method for $r_2 = 0.5$ is shown in Table 7.

C. HEAT TRANSFER IN ANNULAR PASSAGES

Comparisons of the results for heat transfer in annular passages for flow in the fully developed region with Lundberg's [13] and Worsoe-Schmidt's [14] are given in Table 8. For flow in the entrance region, the results compared with Heaton's [19] for the case of uniform heat flux at the inner wall are shown in Table 9. In Heaton's analysis, the effects of v on the flow field are underestimated because of linearization, therefore the Nu numbers obtained by Heaton do not agree very well with the present results. A better agreement is obtained by neglecting v of Eq. (14).
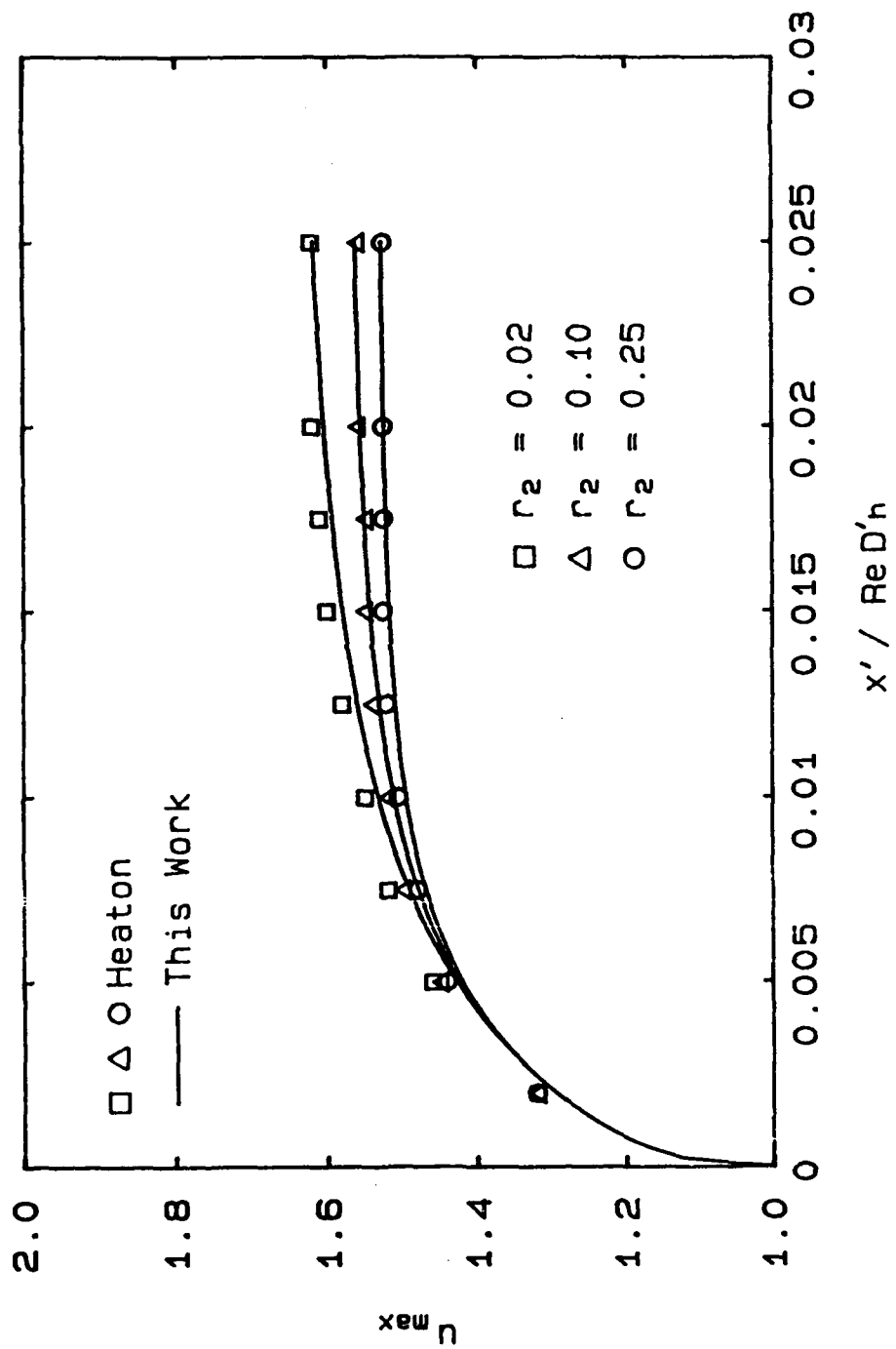
Figure 16. Maximum velocity variation in the entrance region of an annulus

Table 7.   VELOCITY DISTRIBUTIONS IN FULLY DEVELOPED REGION

FOR $r_2 = 0.5$

$\dfrac{r - r_2}{1 - r_2}$	Numerical method		Equation (22)
	11 grids	41 grids	
0.1	0.60266	0.60278	0.60279
0.2	1.03899	1.03912	1.03913
0.3	1.32605	1.32616	1.32616
0.4	1.47716	1.47721	1.47721
0.5	1.50284	1.50283	1.50283
0.6	1.41159	1.41154	1.41153
0.7	1.21036	1.21029	1.21028
0.8	0.90493	0.90485	0.90485
0.9	0.50011	0.50006	0.50006

Table 8. SOLUTIONS OF FLOW IN FULLY DEVELOPED REGION FOR
$r_2 = 0.5$

X	Nu		
	Present	Lundberg	Worsoe-Schmidt
Constant Heat Flux at Inner Wall			
0.0001	34.985	34.6	34.233
0.0010	16.39	16.4	16.356
0.0025	12.378	12.37	12.367
0.005	10.132	10.13	10.127
0.010	8.435	8.433	----
0.025	6.932	6.931	----
0.05	6.353	6.353	----
0.1	6.191	6.192	----
Constant Temperature at Inner Wall			
0.0001	29.802	28.4	28.456
0.0010	13.760	13.68	13.701
0.0025	10.445	10.42	10.427
0.005	8.610	8.602	8.603
0.010	7.249	7.246	7.247
0.025	6.118	6.117	----
0.05	5.784	5.785	----
0.1	5.738	5.738	----

Table 9.   SOLUTIONS OF UNIFORM HEAT FLUX AT INNER WALL FOR

FLOW IN ENTRY REGION WITH $Pr = 10$

X	Nu		
	Present	Neglect v	Heaton
0.0010	16.081	16.468	16.68
0.0025	12.255	12.535	12.60
0.005	10.079	10.187	10.20
0.01	8.414	8.453	8.43

VIII. RESULTS AND DISCUSSION

Figure 17 shows the Nusselt numbers in the thermal entrance region for two cases, one by considering that the flow is fully developed and another case by assuming that the flow field is developing. We see that near the inlet, Nusselt numbers of the developing flow field are larger than those of the fully developed flow field. This is due to the fact that in the velocity developing region, the boundary layer is thinner, therefore the drag force is larger and this makes the Nusselt numbers larger. As the HTF flows down from the inlet, the Nusselt numbers of the two different flow fields become closer.

From Eq. (13) and Eq. (14), one can conclude that the Reynolds number will not affect the local heat flow rates. This is effective only when X is defined by $X = x' \mid Re\ Pr\ D_h$. The effects of changeing the initial temperature of the HTF and the PCM and changing the inlet temperature of the HTF of the thermal storage unit on the Nusselt number are shown to be insignificant.

Figure 18 shows the transient temperature distribution of the PCM for flow in the entrance region. The initial temperature of the PCM and HTF is $38°C$. The inlet temperature of the HTF is $53°C$. Since the temperature of the PCM is initially lower than the melting point temperature, the solid PCM temperature increases to the melting point and melting occurs. However, as time increases, the solid PCM will approach the melting temperature, a constant temperature. The temperature gradient of the PCM at the inner tube wall will decrease with time. This means that the heat flow rate between the HTF and PCM will decrease with time.

The transient temperature distributions of the HTF are shown in Figs. 19 and 20. Near the inlet, the temperature of the HTF is uniform except at the region which is near the outer wall of the PCM tube. For the downstream region, the temperature of the HTF at the center portion between r_2 and r_o is higher than that near the tube wall. This phenomenon is due to the parabolic velocity distribution. However, as time
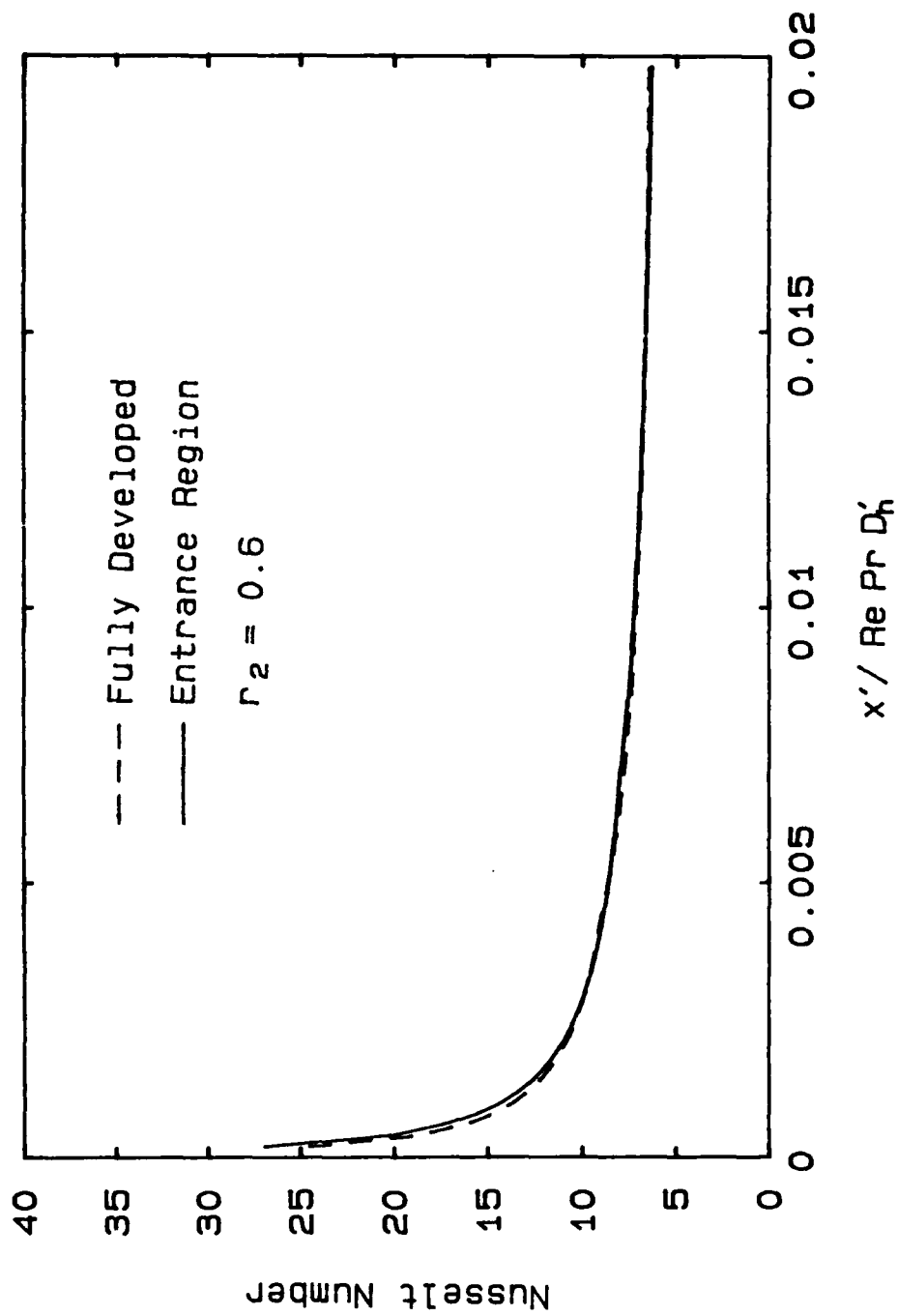
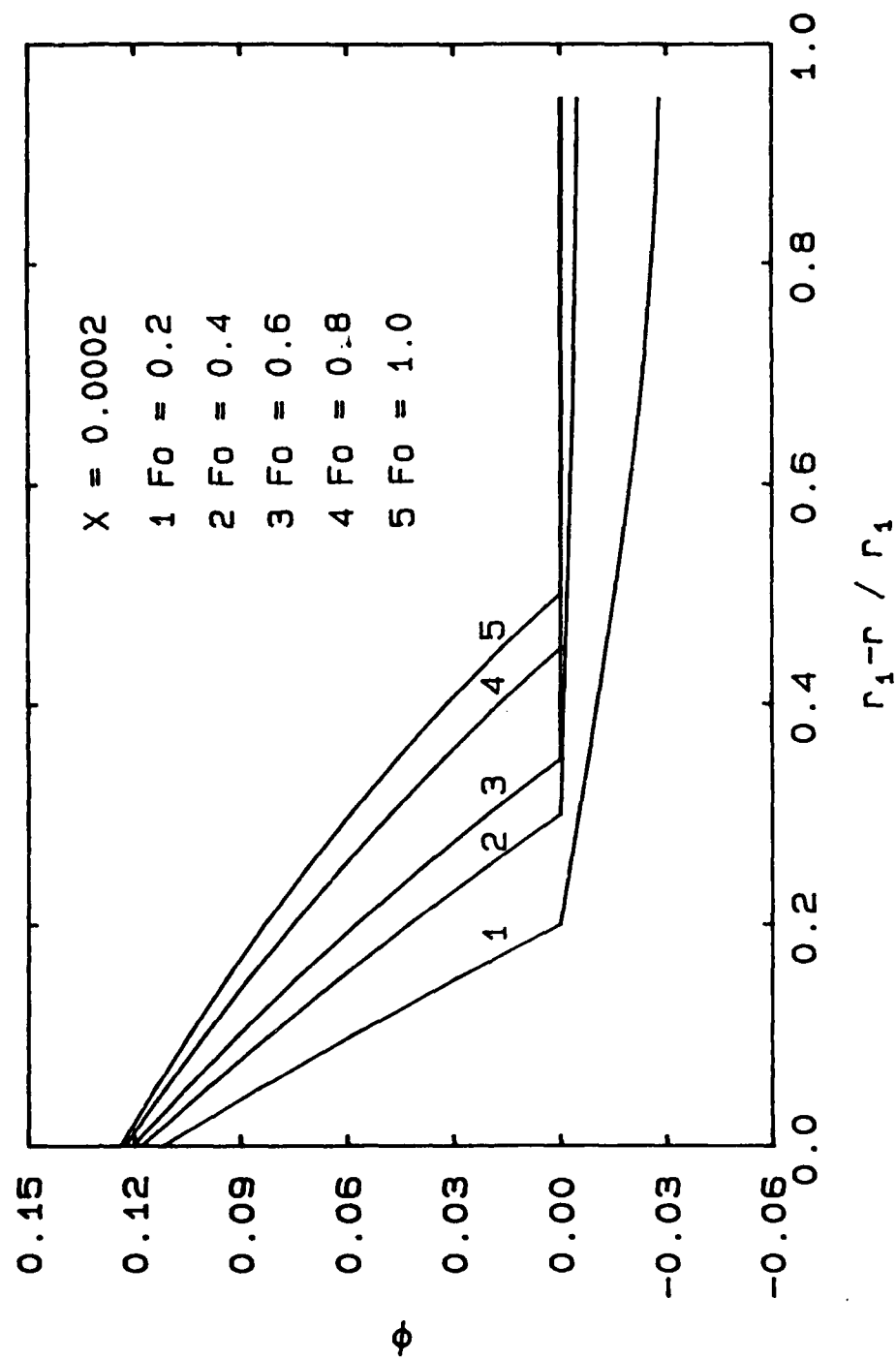Figure 17. Effect of developing velocity profiles on Nusselt number

Figure 18. Temperature distribution of PCM
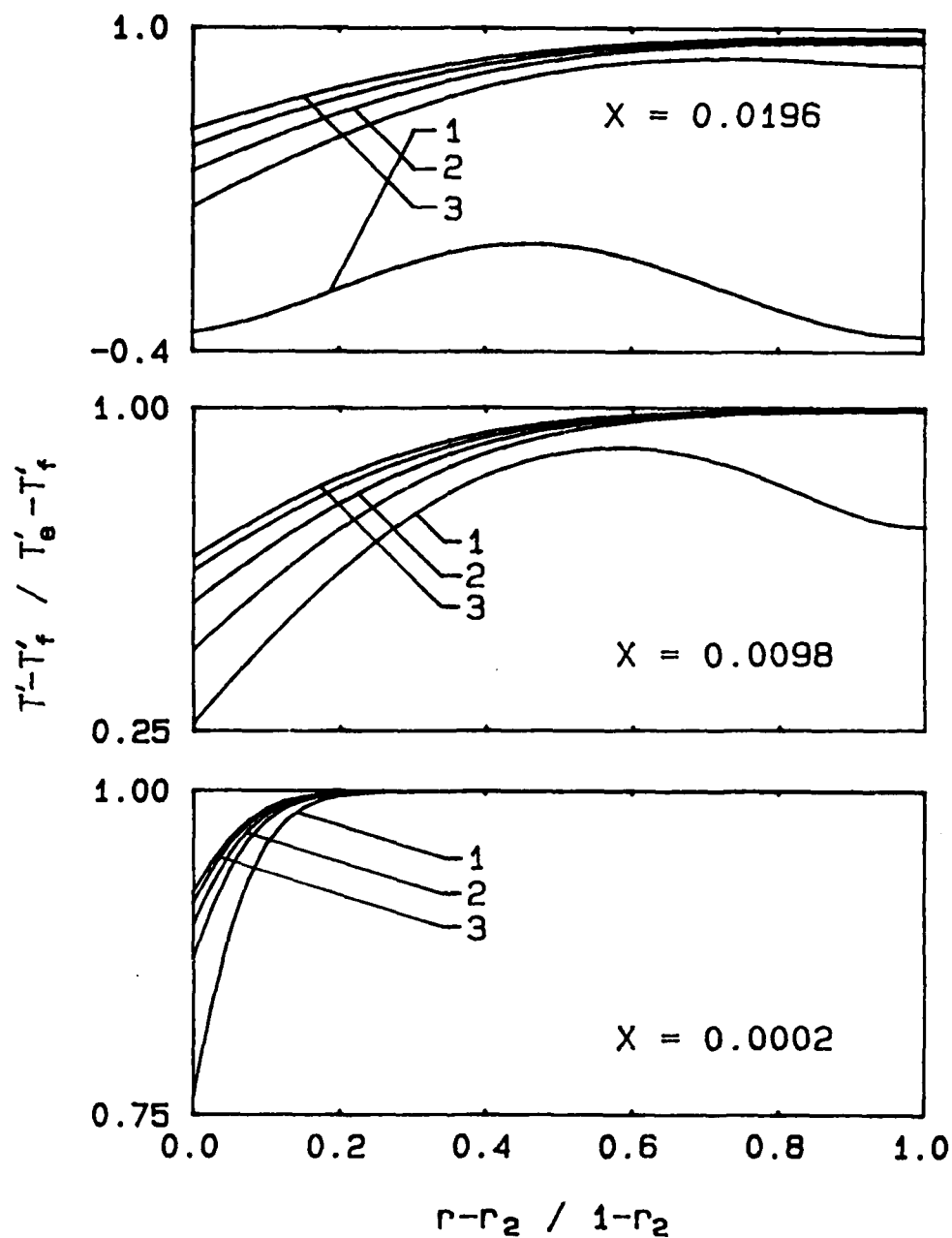
Figure 19. Temperature distribution of HTF in fully developed region for $r_2 = 0.5$
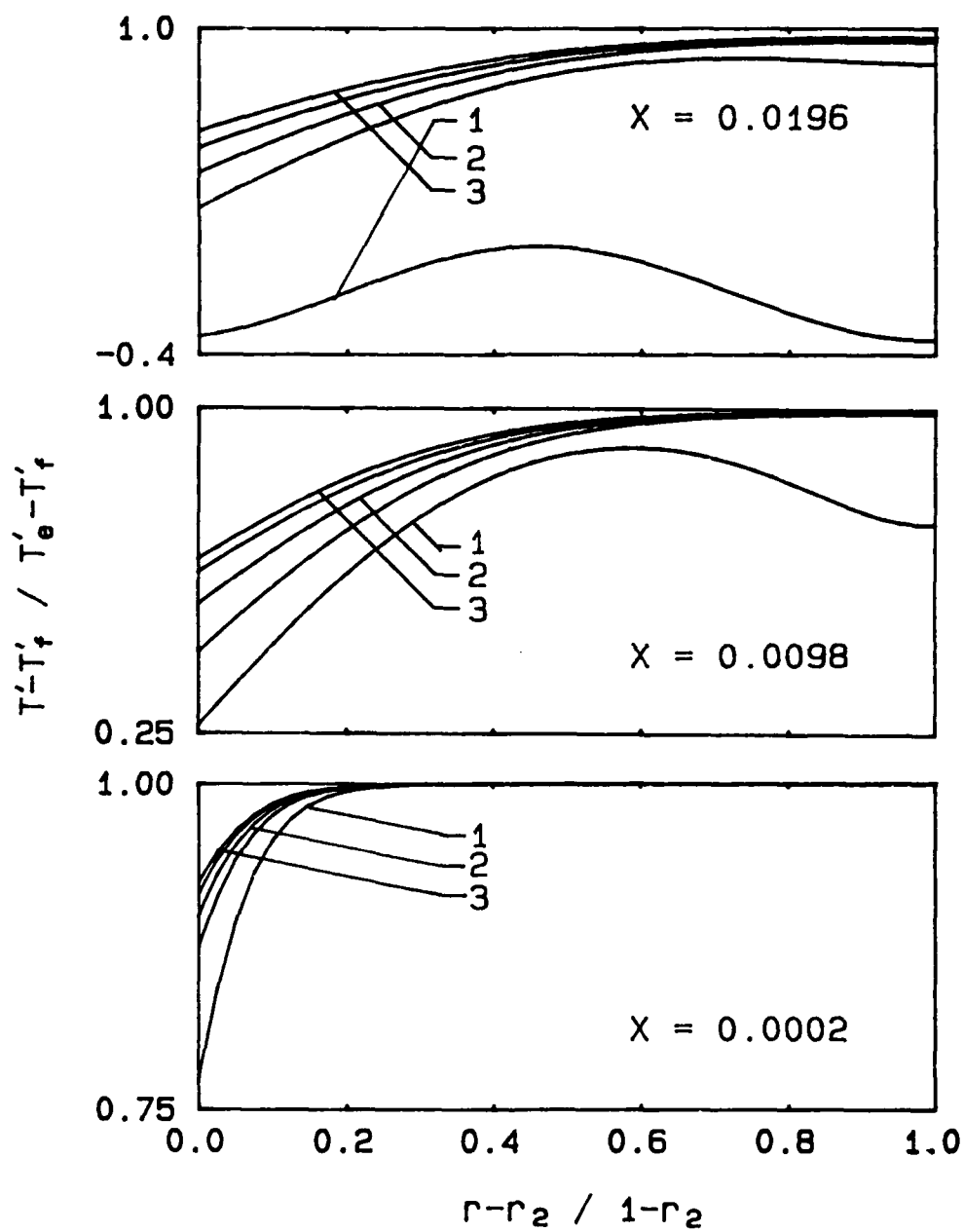(1:Fo = 0.01, 2:Fo = 0.03, 3:Fo = 0.05)

Figure 20.   Temperature distribution of HTF in entrance region for $r_2 = 0.5$
(1:Fo = 0.01, 2:Fo = 0.03, 3:Fo = 0.05)

increases, the temperature gradient appears to be nonzero only at the region which is near to r_2. From Figs. 19 and 20 one would discover that as X decreases, the temperature gradient at r_2 increases. Thus, larger heat flow rates are predicted in the entrance region than in the fully developed region downstream. Note that when time increases, the local heat flow rates decrease.

For melting of the P116 wax in the latent heat storage unit, both experimental data and predicted results showed fair agreement. However, after the experiment progressed 100 minutes, air bubbles generated, which had significant influence on the experimental results, and therefore comparison between the experimental data and predicted results becomes difficult. During the initial melting period, a minimal amount of slumping of the solid PCM was boserved. The end plugs of the PCM capsules offered sufficient thermal resistance ot allow the solid PCM to remain attached to these plugs for a substantial period of the melting process.

The initial time evolution of the solid-liquid interface positions was plotted on Fig. 21 for constant Renolds and Prandtl numbers of 683 and 3.93, respectively. The figure clearly shows that in the upstream region of the HTF, the melting of the PCM is faster than in the downstream region. This is due to the fact that in the upstream region, the temperature of the HTF is higher and both the temperature and velocity profiles are developing. Figure 21 also indicates that the melting is slower as time increases, and this characterizes that the heat flow rates between the HTF and PCM decrease.
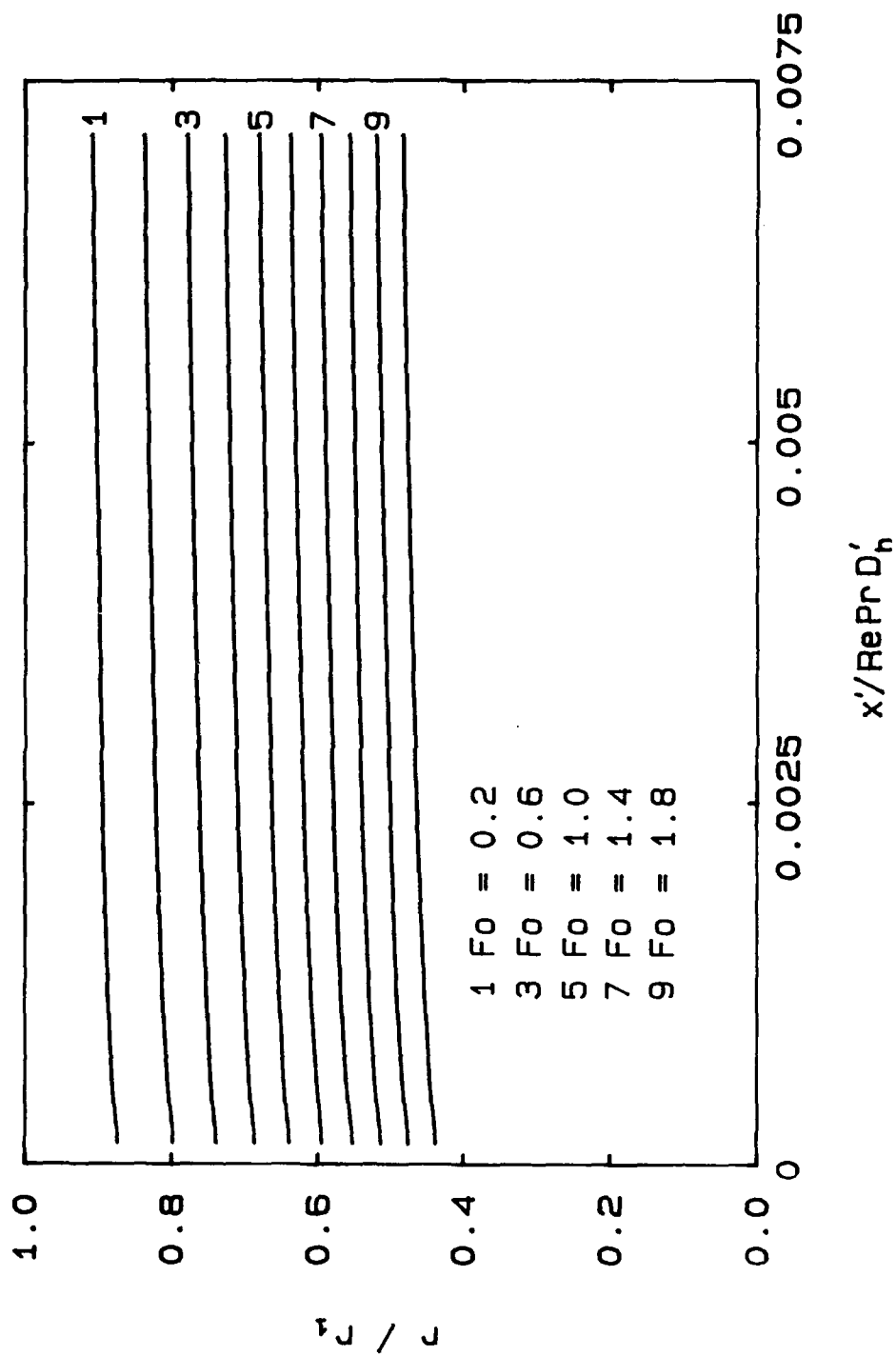
Figure 21. Time evolution of the solid-liquid interface positions for melting of P116 wax

IX. CONCLUSIONS

Analysis and experiments have been performed for a heat transfer study of a latent heat storage unit. Melting/freezing problems were solved by a finite-difference method based on the enthalpy formulation. Convection problems of the HTF were solved by first obtaining the velocity distribution and then by solving the energy equation. In addition to the continuity equation and the momentum equation, the integral continuity equation was also used for calculating the velocity distributions.

From the obtained results one can conclude that: (1) The developing temperature profiles increase the Nusselt number significantly. The developing velocity profiles can also increase the Nusselt number. However, the increase is not so significant when compared with the increase due to the developing temperature profiles. (2) Near the inlet region, the effect of r_2 on the Nusselt number can not be neglected. The Nusselt number increases with the increase of r_2. In the far downstream region, the effect of r_2 on the Nusselt number is small and can be neglected.

REFERENCES

1. B. W. Webb, M. K. Moallemi, and R. Viskanta, "Phenomenology of Melting of Unfixed Phase Change Material in a Horizontal Cylindrical Capsule," ASME paper 86-HT-10, 1986.

2. A. G. Bathelt and R. Viskanta, "Heat Transfer at the Solid-liquid Interface During Melting From a Horizontal Cylinder," Int. J. Heat Mass Transfer Transfer , Vol. 23, 1980, pp. 1493-1503.

3. C. J. Ho and R. Viskanta, "Heat Transfer During Inward Melting in a Horizontal Tube," Int. J. Heat Mass Transfer , Vol. 27, 1984, pp. 705-716.

4. J. Pannu, G. Joglekar and P. A. Rice, "Natural Convection Heat Transfer to Cylinders of Phase Change Material Used for Thermal Storage," AIChE Symposium Series , No. 198, Vol. 76, 1980, pp. 47-55.

5. L. S. Yao and F. F. Chen, "Effects of Natural Convection in the Melted Region Around a Heated Horizontal Cylinder," J. Heat Transfer , Vol. 102, 1980, pp. 667-672.

6. H. Rieger and H. Beer, "The Melting Process of Ice Inside a Horizontal Cylinder: Effects of Density Anomaly," J. Heat Transfer , Vol. 108, 1986, pp. 166-173.

7. H. Rieger, U. Projahn, and H. Beer, "Analysis of Heat Transport Mechanisms During Melting Around a Horizontal Circular Cylinder," Int. J. Heat Mass Transfer , Vol. 25, 1982, pp. 137-147.

8. M. E. McCabe "Periodic Heat Conduction in Energy Storage Cylinders With Change of Phase," ASME Paper 86-HT-12, 1986.

9. E. M. Sparrow and C. F. Hsu, "Analysis of Two-Dimensional Freezing on the Outside of a Coolant-Carrying Tube," *Int. J. Heat Mass Transfer*, Vol. 24, 1981, pp. 1345-1357.

10. N. Shamsundar, "Formulae for Freezing Outside of Circular Tube With Axial Variation of Coolant Temperature," *Int. J. Heat Mass Transfer*, Vol. 25, 1982, pp.1614-1616.

11. S. Asgarpour and Y. Bayazitoglu, "Heat Transfer in Laminar Flow with a Phase Change Boundary," *J. Heat Transfer*, Vol. 104, 1982, pp. 678-682.

12. W. C. Reynolds, R. E. Lundberg and P. A. McCuen, "Heat Transfer in Annular Passages. General Formulation of the Problem for Arbitrarily Prescribed Wall Temperatures or Heat Fluxes," *Int. J. Heat Mass Transfer*, Vol. 6, 1963, pp. 483-493.

13. R. E. Lundberg, P. A. McCuen and W. C. Reynolds, "Heat Transfer in Annular Passages. Hydrodynamically Developed Laminar Flow With Arbitrarily Prescribed Wall Temperatures or Heat Fluxes," *Int. J. Heat Mass Transfer*, Vol. 6, 1963, pp. 495-529.

14. P. M. Worsoe-Schmidt, "Heat Transfer in the Thermal Entrance Region of Circular Tubes and Annular Passages With Fully Developed Laminar Flow," *Int. J. Heat Mass Transfer*, Vol. 10, 1967, pp. 541-551.

15. A. P. Hatton and A. Quarmby, "Heat Transfer in the Thermal Entry Length With Laminar Flow in an Annulus," *Int. J. Heat Mass Transfer*, Vol. 5, 1962, pp. 973-980.

16. W. A. Sutherland and W. M. Kays, "Heat Transfer in an Annulus With Variable Circumferential Heat Flux," Int. J. Heat Mass Transfer , Vol. 7, 1964, pp. 1187-1194.

17. K. Murakawa, "Heat Transfer in Entry Length of Double Pipes," Int. J. Heat Mass Transfer , Vol. 2, 1961, pp. 240-251.

18. N. Liron and J. Gillis, "Stokes Flow in an Annular Region," J. App. Mech. , March 1970, pp. 29-33.

19. H. S. Heaton, W. C. Reynolds and W. M. Kays, "Heat Transfer in Annular Passages. Simultaneous Development of Velocity and Temperature Fields in Laminar Flow," Int. J. Heat Mass Transfer , Vol. 7, 1964, pp. 763-781.

20. H. Lamb, "Hydrodynamics," 5th Ed., Cambridge University Press , 1924.

21. C. Wen, J. W. Sheffield, M. P. O'Dell and J. Leland, "An Analytical and Experimental Investigation of Melting Heat Transfer," AIAA Paper 88-0357, 1988.

22. R. Viskanta and C. Gau, "Inward Solidification of a Superheated Liquid in a Cooled Horizontal Tube," Warme-und Stoffubertragung , Vol. 17, 1982, pp.39-46.

LIST OF ACRONYMS

A/D	Analog to Digital
DSC	Differential Scanning Calorimetry
HQ	High Quality
HTF	Heat Transfer Fluid
PCM	Phase Change Material
SCTMS	Spacecraft Thermal Management Systems
VCR	Video Cassette Recorder

LIST OF SYMBOLS

A,   area

A_1,   constant

A_2,   constant

A_3,   constant

B,   constant

c,   specific heat

C,   constant

D',   diameter

D'_h,   hydraulic diameter, $2(r'_o - r'_2)$

h,   heat transfer coefficient

i,   specific enthalpy

k,   thermal conductivity

L',   length of tube

M,   constant

p',   pressure

Q,   heat flow per length

Q_{x1},   local heat flow per length

Q_{x2},   local heat flow per length

q,   heat flow rate

r',   spatial coordinate

T,   temperature

t,   time

U,   specific internal energy

u',   axial component of velocity

v',   radial component of velocity

x',   spatial coordinate

LIST OF SYMBOLS (Continued)

Greek symbols

α,   thermal diffusivity

λ,   latent heat of fusion

ρ,   density

υ,   kinematic viscosity

ϵ ,   convergence criteria

Δ,   step size

Dimensionless quantities

Fo,   Fourier number, dimensionless time, Eq.(7)

L,   length of tube, $L' / Re\,Pr\,D'_o$

Nu,   Nusselt number

p,   pressure, $p' / (\rho\,u'^2_m / 2)$

Pr,   Prandtl number, υ/α

Re,   Reynolds number, $u'_m\,D'_h / \upsilon$

Re',   Reynolds number, $2u'_m\,r'_o / \upsilon$

r,   spatial coordinate, r'/r'_o

Ste,   Stefan number, Eq.(39)

T,   temperature, $(T' - T'_f)/(T'_e - T'_f)$

u,   axial component of velocity

v,   radial component of velocity

X,   spatial coordinate, $x'/Re\,Pr\,D'_h$

x,   spatial coordinate, $x'/Re'\,r'_o$

χ,   spatial coordinate, x'/r'_1

Z,   spatial coordinate, $x'/Re\, r'_o$

θ,   enthalpy, Eq.(5)

$\tilde{\theta}$,   scaled dimensionless enthalpy, Eq.(28)

ϕ,   scaled dimensionless temperature, Eq.(8)

τ,   dimensionless time, $\alpha_h\, t\, /\, r'^2_o$

Subscripts

b,   mean bulk value

e,   at the inlet

f,   fusion

h,   heat transfer fluid

i,   spatial location

ini,   initial value

j,   spatial location

l,   liquid region

m,   mean value

max,   maximum value

o,   at the shell wall

p,   phase change material

t,   tube

1,   at the inner-wall of tube

2,   at the outer-wall of tube

Superscripts

m,	time level
*,	saturated state